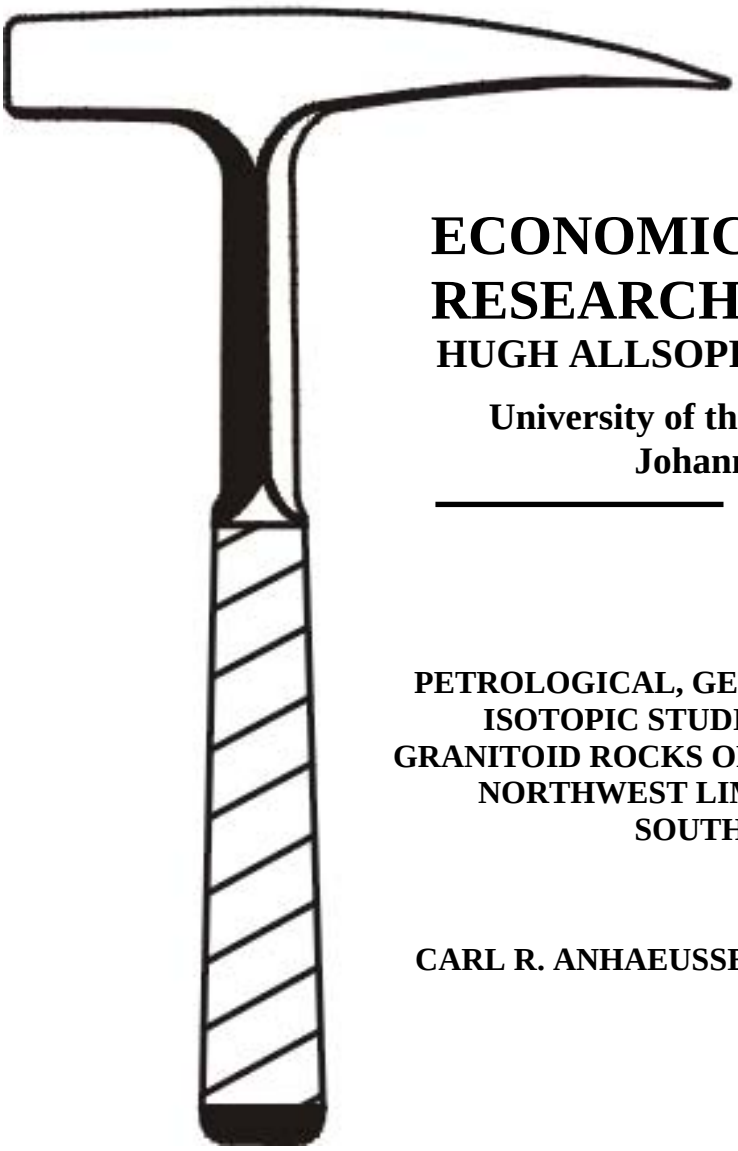

ECONOMIC GEOLOGY RESEARCH INSTITUTE

HUGH ALLSOPP LABORATORY

University of the Witwatersrand
Johannesburg

PETROLOGICAL, GEOCHEMICAL AND U-Pb ISOTOPIC STUDIES OF ARCHAEAN GRANITOID ROCKS OF THE MAKOPPA DOME, NORTHWEST LIMPOPO PROVINCE, SOUTH AFRICA

CARL R. ANHAEUSSER and MARC POUJOL

INFORMATION CIRCULAR No. 372

UNIVERSITY OF THE WITWATERSRAND
JOHANNESBURG

PETROLOGICAL, GEOCHEMICAL AND U-Pb ISOTOPIC STUDIES OF ARCHAEAN GRANITOID ROCKS OF THE MAKOPPA DOME, NORTHWEST LIMPOPO PROVINCE, SOUTH AFRICA

by

C.R. ANHAEUSSER[1] AND M. POUJOL[2]

([1]Economic Geology Research Institute, School of Geosciences, University of the Witwatersrand, Private Bag 3, P.O. WITS 2050, Johannesburg, South Africa.
[2] Department of Earth Sciences, University of Newfoundland, St John's, Newfoundland, NF A1B 3X5, Canada)

ECONOMIC GEOLOGY RESEARCH INSTITUTE
INFORMATION CIRCULAR No. 372

November, 2003

PETROLOGICAL, GEOCHEMICAL AND U-Pb ISOTOPIC STUDIES OF ARCHAEAN GRANITOID ROCKS OF THE MAKOPPA DOME, NORTHWEST LIMPOPO PROVINCE, SOUTH AFRICA

ABSTRACT

The Makoppa Dome, located in the far northwestern part of the Kaapvaal Craton, constitutes one of the least well-exposed Archaean granite-greenstone terranes in southern Africa. For this reason it has received very little attention in the past and its characteristics have largely gone undocumented. This study presents new field, petrological, geochemical and single zircon dating results for a suite of granitoid rocks that comprise foliated trondhjemitic gneisses and homogeneous monzogranitic, adamellitic and granodioritic phases, all of which postdate remnants of Archaean greenstone belts metamorphosed to amphibolite facies. Three separate granitoid types are recognized on the basis of their distinctive field as well as major, trace and rare-earth element characteristics. Confirmation of the three granite-types follows from new ID-TIMS and LAM-ICP-MS dating of single zircons extracted from samples collected on the dome. The oldest granitoid rocks so far recognized are represented by the Vaalpenskraal-type trondhjemitic gneisses, two samples of which yielded ages that are identical within error and are dated at 3011+30/-29 Ma and 3034±64 Ma respectively. A single sample of homogeneous monzogranite/adamellite, referred to as Makoppa-type granitoid, yielded an age of 2886.4+3/-2.3 Ma, while a further two samples of homogeneous granodiorite, referred to as Rietkuil-type granitoid, are representative of the youngest granitic event recorded on the dome and yielded ages of 2801±24 Ma and 2796.8±2.4 Ma respectively. The Makoppa Dome granitoids have many features in common with those of the Kraaipan-Amalia terrane on the western side of the Kaapvaal Craton as well as those of the Murchison-Giyani-Pietersburg terrane on the northern side, supporting suggestions that these rocks developed in or adjacent to a crescent-shaped magmatic arc that began forming *c.*3100-3000 Ma ago around the northern, northwestern and western rim of the Kaapvaal Craton. Continent-arc collision followed in the period up to approximately 2800 Ma, the time of emplacement of the Rietkuil granitoids on the Makoppa Dome and the *c.* 2791±8 Ma Mosita granitoids in the Kraaipan terrane. These ages closely approximate the age of the *c.* 2785 Ma Gaborone Granite Complex in neighbouring Botswana and may represent the proto-magmatic stages leading to the development, on thickened crust, of the A-type Gaborone granite suite and Kanye volcanic formation, followed, in turn, by the rift-related *c.* 2714 Ma volcanism of the Ventersdorp Supergroup.

_____oOo_____

PETROLOGICAL, GEOCHEMICAL AND U-Pb ISOTOPIC STUDIES OF ARCHAEAN GRANITOID ROCKS OF THE MAKOPPA DOME, NORTHWEST LIMPOPO PROVINCE, SOUTH AFRICA

CONTENTS

_____oOo_____

Published by the Economic Geology Research Institute
(incorporating the Hugh Allsopp Laboratory)
School of Geosciences
University of the Witwatersrand
1 Jan Smuts Avenue
Johannesburg
South Africa

http://www.wits.ac.za/geosciences/egri.htm

ISBN 1-86838-331-8

PETROLOGICAL, GEOCHEMICAL AND U-Pb ISOTOPIC STUDIES OF ARCHAEAN GRANITOID ROCKS OF THE MAKOPPA DOME, NORTHWEST LIMPOPO PROVINCE, SOUTH AFRICA

INTRODUCTION

Archaean granitoid rocks of the Kaapvaal Craton have formed the subject of a number of investigations aimed at determining the geological, geochemical and geochronological character and evolutionary history of the early crust of southern Africa. The most extensively studied exposures of basement granitoids, which comprise gneisses, migmatites and a range of rocks of granitic (*sensu lato*) composition (i.e., diorites, tonalities, trondhjemites, granodiorites, adamellites/ monzogranites) and granites (*sensu stricto*) occur in the Mpumalanga Lowveld and Swaziland regions on the eastern side of the Kaapvaal Craton (the ***eastern domain*** *[ED]* of Poujol *et al.*, 2003 - see Figure 1 inset map). Descriptions of these rocks, which are best developed to the north and south of the Barberton greenstone belt, include those of Hunter (1970, 1973, 1974), Anhaeusser and Robb (1980, 1981, 1983a), Anhaeusser *et al*. (1981, 1983), Robb (1983), Robb and Anhaeusser (1983), Robb *et al*. (1983) and Meyer *et al*. (1994).

This predominantly TTG suite of granitoid rocks in the eastern domain ranges in age from *c*. 3700 to 2725 Ma (Kamo and Davis, 1994; Kröner *et al*., 1996; Poujol *et al*., 2003). Within this time frame at least four main episodes involving tectonic accretion (Lowe, 1994) and granitoid magmatism have been recognized at 3545-3490, 3490-3420, 3255-3225 and 3105-3070 Ma, with minor, discrete events occurring around 3325-3310, 2985 and 2725Ma, respectively (Poujol *et al*., 2003). Regional geochemical studies (Hunter *et al*., 1978; Anhaeusser and Robb, 1983b) further demonstrated that there was a progressive change with time in the composition of the granitoids from essentially sodium-rich tonalitic and trondhjemitic gneisses and migmatites (*c*. 3550 - 3200 Ma) to more potassium-rich granodiorites, adamellites and granites (*c*. 3200 - 2700 Ma).

Archaean TTG granitoid rocks have also been studied in the northern, central and western domains of the Kaapvaal Craton (Figure 1) where they yielded younger ages relative to the Barberton-Swaziland granitoids of the eastern domain. These later granitoid rocks, it has been argued, represent either crustal additions resulting from episodes of magmatic accretion (Poujol *et al*., 2003), or the tectonic amalgamation of small protocontinental blocks (De Wit *et al*., 1992).

Granitic rocks from the ***northern domain*** *(ND,* Figure 1 inset map) in the vicinity of the Murchison, Pietersberg and Giyani/Sutherland greenstone belts, yield ages ranging from *c*. 3364-2674 Ma (Brandl and Kröner, 1993; Poujol, 2001; Poujol and Robb, 1999; Poujol *et al*., 1996, 2003; Henderson *et al*., 2000; Kröner *et al*., 2000). The oldest granitoids consist of Palaeoarchaean trondhjemite-tonalite gneisses and migmatites (*c*. 3333-3230 Ma), followed by largely post-tectonic Meso- to Neoarchaean granitoid intrusions in the Polokwane (formerly Pietersburg) and Murchison areas (*c*. 3200-2674 Ma). These rocks consist mainly of massive, unfoliated, potassic granitoids (granodiorite to adamellite/monzogranite) that occur as batholiths or plutons and generally form prominent topographic features in the Polokwane area.

Archaean granitoid rocks of the ***central domain*** *(CD,* Figure 1 inset map*)* are confined to exposures located on the Johannesburg and Vredefort Domes, as well as along the Rand

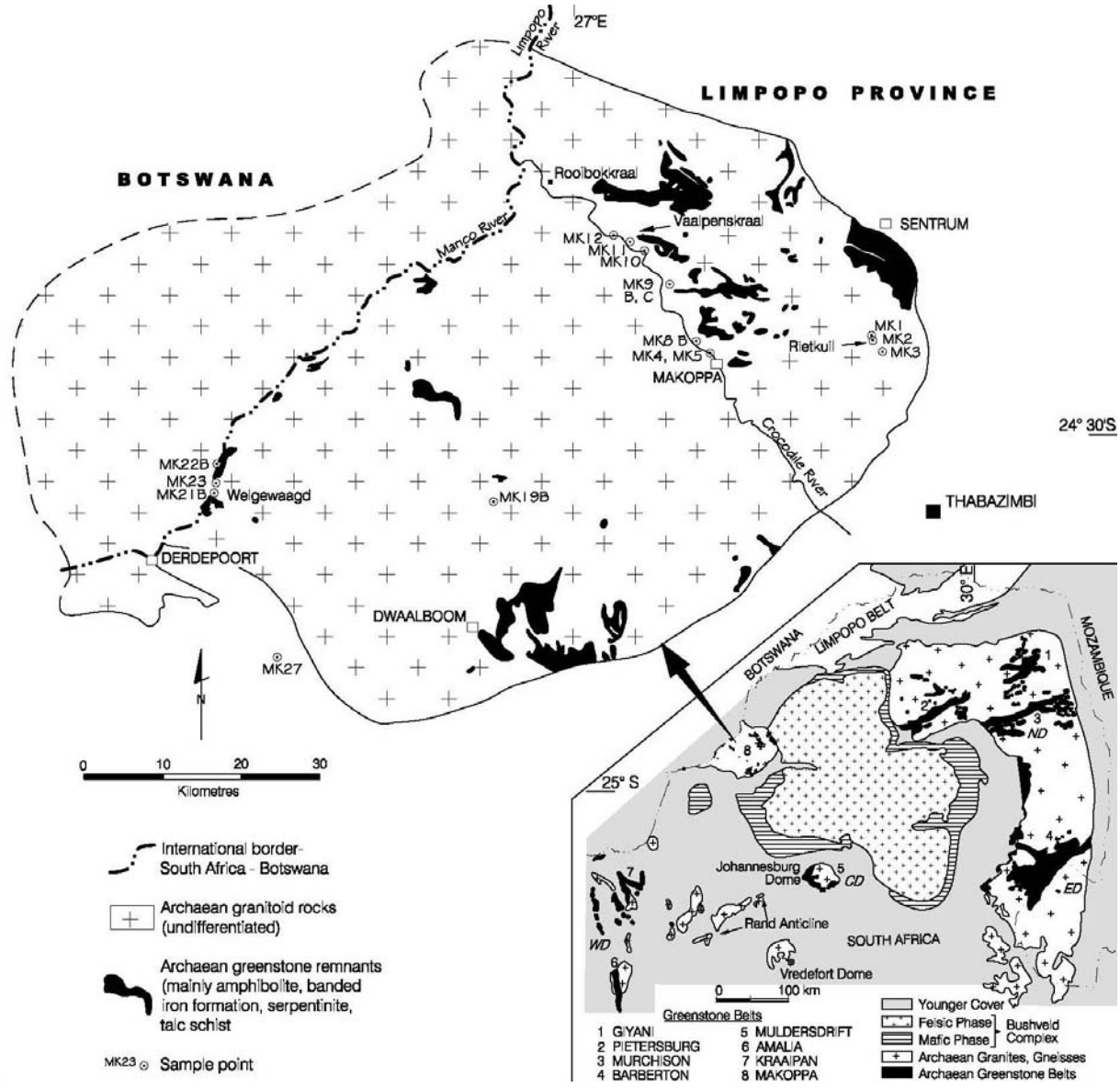

Figure 1. *Simplified geological map of the Makoppa Dome showing the localities of samples studied in this paper. The inset map, lower right, shows the main exposures of Archaean granite-greenstone basement rocks on the Kaapvaal Craton.*

Anticline extending southwest of Johannesburg (Anhaeusser, 1973b; Robb and Meyer, 1987; Drennan *et al*., 1990; Bisschoff, 2000; Gibson and Reimold, 2001). Other information on the central domain granitoids has been derived from Witwatersrand gold exploration boreholes.

The Archaean basement granitic rocks of the central domain range in age from *c*. 3340-2727 Ma (Hart *et al*., 1981; Anhaeusser and Burger, 1982; Armstrong *et al*., 1991; Barton *et al*., 1999; Moser *et al*., 2001; Poujol and Anhaeusser, 2001; Robb *et al*., 1992). As summarized by Poujol *et al*. (2003) the U-Pb geochronological data in this region define three main peaks at 3200-3175, 3120-3075 and 2730-2705 Ma.

The Johannesburg Dome represents the best-exposed granite-greenstone basement inlier in the central domain. A number of magmatic events responsible for the development of the crust in this region have been recognized, including volcanic and plutonic rocks of mafic and ultramafic affinity found as greenstone xenoliths on the dome and a suite of tonalite-trondhjemite-granodiorite/adamellite granitoid rocks shown to intrude the greenstones causing their fragmentation, metamorphism, metasomatism, assimilation and migmatization (Anhaeusser, 1973a,b, 1992, 1999).

The oldest granitoid phase recognized is a trondhjemitic gneiss from the northwestern part of the Johannesburg Dome that yielded an age of *c*. 3340 Ma (Poujol and Anhaeusser, 2001). On the south side of the dome hornblende-tonalite gneisses intruded at *c*. 3200-3170 Ma (Anhaeusser and Burger, 1982; Poujol and Anhaeusser, 2001). A younger suite of potassic granitoids comprising mainly homogeneous and, in places, porphyritic granodiorites/adamellites ranging in age between *c*. 3121 and 3114 Ma occupy the central parts of the dome (Poujol and Anhaeusser, 2001). A Pb-Pb zircon age of *c*. 3090 Ma was recorded for similar rocks in this area by Barton *et al*. (1999) and pegmatite dykes and veins, some possibly as young as 3000 Ma, crosscut all earlier granitic phases (Poujol and Anhaeusser, 2001).

Ages ranging between *c*. 3200-2727 Ma have also been recorded from granitoid rocks of the Vredefort Dome, the Rand Anticline, and borehole samples as far as 250 km southwest of Johannesburg (Drennan *et al*., 1990; Armstrong *et al*., 1991; Robb *et al*., 1992).

The Archaean basement rock of the ***western domain*** (*WD*, Figure 1 inset map) crop out sporadically from Botswana in the north to Kimberley in the south, a distance of about 400km. Greenstone belt successions in the Amalia-Kraaipan areas (Figure 1 - inset map) consist predominantly of northwest-trending metasediments, including banded iron formations, jaspilites, cherts and breccias as well as a variety of metavolcanic mafic and ultramafic schists (Van Eeden *et al*., 1963; SACS, 1980; Zimmermann, 1994). These are, in turn, intruded by a suite of granitoid rocks comprising TTG gneisses, granodiorites and adamellites ranging in age from *c*. 3250-2718 Ma (Drennan *et al*., 1990; Robb *et al*., 1992; Anhaeusser and Walraven, 1999; Poujol *et al*., 2002).

The oldest basement rocks in the western domain occur in mine exposures and borehole intersections in the Kimberley region, about 110km south of Amalia, and consist of gneissic to migmatitic tonalitic to granodioritic rocks dated at *c*. 3250 Ma (Drennan *et al*., 1990). Further north, in the Amalia-Kraaipan-Madibe areas, a suite of granitoid rocks ranging in age from *c*. 3200-2790 Ma have been recorded (Anhaeusser and Walraven, 1999; Gericke, 2001;

Poujol *et al*., 2002). As with the examples described elsewhere on the Kaapvaal Craton the oldest granitoids consist of TTG gneisses and migmatites while later, potassic, homogeneous and porphyritic granodiorite/adamellite phases record ages ranging between *c*. 2915-2880 Ma (Drennan *et al*., 1990; Anhaeusser and Walraven, 1999; Poujol *et al*., 2002; Schmitz *et al*., 2003). The youngest granitoid rocks occur west of Kraaipan where the Mosita adamellite pluton has yielded ages ranging between *c*. 2718 and 2791Ma (Burger and Walraven, 1979; Anhaeusser and Walraven, 1999; Poujol *et al*., 2002).

The Makoppa Dome, located in the northwest segment of the Limpopo Province, and straddling the border between South Africa and Botswana, occupies an area approximately 7600km^2 in extent. Of this total about 5000km^2 of the dome occurs in South Africa. Due to poor exposure, however, the Makoppa Dome has not been studied in detail and no distinction has been attempted of the granitoid rocks in the region. Currently, the best available information is that shown on the 1:250 000 map (Geological Series 2426 Thabazimbi) compiled by Jansen *et al*. (1974). A total magnetic field intensity map (1:250 000 Regional Aeromagnetic Series 2426 Thabazimbi) highlights the NW-SE trending Pilanesburg dyke swarm that intrudes the Makoppa Dome (CFG, 1975).

The present study is aimed at presenting new petrological, geochemical and U-Pb isotopic data pertaining to the granitoid rocks of the Makoppa Dome and to accommodate the findings within a model proposed by Poujoil *et al.* (2003) suggesting the presence of a crescent-shaped arc that was accreted onto the northern and western margins of the evolving Kaapvaal Craton approximately 3100-3000 Ma ago and which was, in turn, further influenced by magmatism associated with continent-arc collision between 3000 and 2700 Ma adjacent to the craton margins.

GENERAL GEOLOGY OF THE MAKOPPA DOME

The Archaean granite-greenstone terrane defining the Makoppa Dome is enveloped by Neoarchaean and Eoproterozoic volcanic and sedimentary rocks of the Kanye/Ventersdorp (?) and Transvaal Supergroups in the southwest, south and southeast, and by Palaeoproteozoic sediments of the Waterberg Supergroup in the north and northeast (Jansen *et al*., 1974; Tyler, 1979a, b, c; Wingate, 1998). Bushveld granites abut against the Archaean basement rocks north of Thabazimbi and southeast of Sentrum (Figure 1, inset map). An outlier of chromiferous pyroxenite, believed to be similar to pyroxenites from the Lower Zone of the Bushveld Complex (Jansen *et al*., 1974; Anhaeusser, 2002a) provides one of the few positive topographical features on the dome and forms a line of hills, known as ‘Koringkoppies’, which extend for over 1km in an east-west direction and displays pseudostratification dipping approximately 30ºS. Post-Waterberg diabases, granophyric gabbros and granophyric rocks occur as sill-like intrusions in the areas flanking the northern and northeastern parts of the dome. In the southwest granitoid rocks associated with the Gaborone Granite Complex are restricted to the area southeast and southwest of Derdepoort (Figure 1). The Makoppa Dome extends westwards into the Kgatleng District of neighbouring Botswana where it is intruded in the west by the Gaborone Granite Complex and overlain in the north by red conglomerates, sandstones and shales of the Waterberg Supergroup (Mortimer, 1984).

The Kanye/Ventersdorp (?) and Transvaal Supergroup rocks dip to the south off the dome at angles varying from 20 to 60º, while the Waterberg sediments and the post-Waterberg igneous rocks occur subhorizontally and do not appear to have been tectonically influenced by the

doming event. Numerous NW-SE trending dykes, thought by Jansen *et al*. (1974) to be linked to the Pilanesberg dyke system, are intruded into the Archaean basement granitoids, but are rarely exposed. Their presence as a dyke swarm is, however, reflected on the 1: 250 000 scale aeromagnetic map of the dome (CFG, 1975).

Archaean granite-greenstone basement exposures on the dome are extremely poor as the area is covered by large tracts of Tertiary to Quaternary calcrete, surface limestone, gravel and Kalahari sand. The region is covered by dense bushveld and access is rendered difficult because land use is principally for game farming. In this study the best granitoid exposures were found along the Crocodile River and in the Rietkuil area in the northeastern sector of the dome (Figure 1). The northwest-trending Crocodile River occupies a major reactivated fault parallel to the strike of the Pilanesberg dyke swarm. Incision of the river below the surficial cover has exposed granitic rocks in places between Makoppa and Rooibokkraal (Figure 1).

Archaean greenstone remnants occur scattered across the dome, but are rarely exposed. Their presence is generally detected by changes in soil colour and surface float, the latter comprising mainly amphibolite, banded iron-formation, serpentinite and talc/chlorite schist. Most of the greenstone localities occur northeast of the Crocodile River (between Makoppa and Vaalpenskraal and south of Sentrum) and in the region southeast of Dwaalboom (Jansen *et al*., 1974). Amphibolites, some garnet-bearing, are exposed along the Botswana border in the Welgewaagd area and to the northeast along the Marico River (Figure 1).

GRANITOID ROCKS

Field investigations, particularly along the Crocodile River and adjacent areas to the northeast, have led to the recognition of three varieties of granitoid rocks on the Makoppa Dome (Anhaeusser, 2002b). These include: (1) grey, medium- to coarse-grained, in places weakly foliated and/or banded gneissic granitoids, which mostly display a subhorizontal foliation (*Vaalpenskraal-type gneisses*); (2) reddish, coarse-grained, homogeneous, porphyritic granitoids, the latter intruded by fine-grained, reddish-coloured aplitic dykes and coarser-grained pegmatite dykes (*Makoppa-type granodiorites*); and (3) grey to pinkish-grey, medium- to fine-grained, homogeneous, in places porphyritic granitoids (*Rietkuil-type granodiorites*). In some places, particularly in the Vaalpenskraal and to a lesser extent in the Welgewaagd areas (Figure 1) the gneissic granitoids have been intruded by dykes and sheets of homogeneous granodiorite and pegmatite, considered here to be mostly equivalents of the Makoppa-type granitoids. By contrast the Rietkuil granitoids, which are well-exposed in a number of tor-like exposures on the farm Rietkuil 101KQ (Figure 1), show no signs of any aplitic or pegmatitic phases, and field relationships with respect to the other granitoids cannot be determined directly.

Petrology and geochemistry

Vaalpenskraal-type trondhjemitic gneisses

The gneisses of the Makoppa Dome are best exposed in the Vaalpenskraal area along the north bank of the Crocodile River (see Figure 1 for sample localities). Other sample sites include those in the Welgewaagd area (MK 21B, MK 22B), approximately 15 km northeast of Derdepoort and on the farm Engeland 183KP situated about 16km north of Dwaalboom (MK

Figure 2. *(A) Trondhjemitic gneisses of the Vaalpenskraal-type exposed on the farm Engeland 183KP north of Dwaalboom, showing stromatic layers consisting of alternating pegmatoid or granitoid leucosomes and grey, biotite-rich melanosomes. (B) Banded trondhjemitic gneisses from same locality as (A) showing coarse-grained, strongly foliated stromatic layering (1) and fine-grained, foliated, grey gneiss (2) crosscut by a quartz-rich pegmatoid dyke. (C) Platform exposures of Makoppa-type granodiorite exposed downstream of the bridge and weir straddling the Crocodile River near the settlement of Makoppa. Pegmatites and aplitic dykes intrude the homogeneous, reddish-coloured, coarse porphyritic granodiorites at this locality. (D) Close-up view of the homogeneous, porphyritic Makoppa-type granodiorite at locality (C). Keys for scale. (E) Homogeneous, coarse-grained, reddish-coloured, pegmatite dyke intruding the porphyritic Makoppa-type granodiorite at locality (C). (F) Homogeneous, medium-grained, greyish-pink Rietkuil-type granodiorite forming tor exposures on the farm Rietkuil 101KQ. The granodiorite is porphyritic in places, but no pegmatitic phase was seen at this or other Rietkuil granodiorite localities.*

19B). The gneisses, which are generally grey in colour, are either foliated or show stromatic layering comprising alternating pegmatoid or granitoid leucosomes and darker-coloured melanosomes containing mainly biotite, plagioclase and quartz. Crosscutting dykes of pegmatitic or granitic material are also common (Figure 2A, B).

The grey gneisses are trondhjemites containing mainly quartz, albitic plagioclase and biotite as well as accessory amounts of microcline, perthite, apatite, zircon, magnetite and ilmenite. The plagioclase is variably saussuritized and sericitized to epidote, sericite and muscovite and rutile needles occur in some of the biotite crystals.

Whole-rock major and trace element analyses of the Makoppa granitoid samples were by determined by X-ray fluorescence in the Department of Geology at the University of the Witwatersrand, Johannesburg, using fused glass discs and pressed powder pellets, respectively. REE for some of the samples were analysed using the ICP-MS facility in the Department of Geological Sciences at the University of Cape Town. CIPW norms were calculated using Minpet Version 2.0 software. The geochemical data are presented in Table 1, which shows the three categories of Makoppa granitoid rocks. Average values for the granitic rocks of each category are also listed, together with analyses of a late reddish-coloured aplitic dyke (MK4), which intrudes the Makoppa-type granodiorites at sample locality MK5. Sample MK27, from a locality approximately 25km WSW of Dwaalboom (Figure 1), represents a granitic rock from the Gaborone Granite Complex, and has been included here for comparative purposes.

Table 1 (columns 1-7) lists the composition of trondhjemitic gneisses from seven localities on the dome. The gneisses are distinguished by their high Na_2O and Sr and low K_2O and Rb contents relative to the other granitoid varieties listed. Harker-type variation diagrams displaying the relative abundances of both major and trace element data for all varieties of the Makoppa Dome granitoid rocks are shown in Figures 3 and 4. The spread of values shown by the trondhjemite data may be related to contamination or metasomatism resulting from the intrusion of the later more potassic granitoids. A degree of selective recrystallization of the trondhjemites may also have occurred causing major and trace element mobility. This recrystallization, whether by metamorphic or magmatic causes, appears to have selectively influenced the Zr distribution in the gneisses resulting in crystal zonation and the consequent spread of data used for dating the rocks (see later geochronology).

The trondhjemites of the Makoppa Dome show variations in Al_2O_3 content that are both greater and less than ~15% - a value used by Barker (1979) to distinguish trondhjemites as high-and low-Al_2O_3 types. Arth (1979) also used Al_2O_3 values of 14.5-15% to distinguish between trondhjemites originating in continental environments (> 14.5-15%) and oceanic environments (< 14.5-15%). However, Archaean trondhjemites from a variety of settings on the Kaapvaal Craton, including the Johannesburg, Barberton and Kraaipan-Amalia regions (Anhaeusser, 1973b, 1999; Anhaeusser and Robb, 1980, 1983b; Anhaeusser and Walraven, 1999) contain both types, often side by side or in close proximity, thereby making any inferences as to the environmental setting, based solely on Al_2O_3 content, somewhat subjective.

REE data (Table 1), normalized to chondrite abundances, are shown in Figure 5. Three of the trondhjemite samples analysed display steep REE patterns with strong LREE enrichment and moderate to strong HREE depletion (Figure 5A).The patterns show considerable fractionation

Table 1 Selected granitoid analyses from the Makoppa Dome, northwest Limpopo Province

Category	I	Vaalpenskraal-type trondhjemitic gneisses							II	Makoppa-type granodiorite/adamellite				III	Rietkuil-type granodiorite			IV	Gaborone
Column	1	2	3	4	5	6	7	8	9	10	11	12	13	14	15	16	17	18	19
Sample	MK-9C	MK-10	MK-11	MK-12	MK-19B	MK-21B	MK-22B	X-I	MK-5	MK-8B	MK-9B	MK-23	X-II	MK-1	MK-2	MK-3	X-III	MK-4	MK-27
SiO_2	69.69	71.75	72.32	74.52	75.38	73.29	71.45	72.63	73.3	73.26	72.41	73.37	73.09	72.96	73.83	73.38	73.39	68.89	78.01
TiO_2	0.38	0.29	0.27	0.08	0.04	0.17	0.07	0.19	0.21	0.2	0.36	0.08	0.21	0.25	0.23	0.24	0.24	0.11	0.25
Al_2O_3	16.33	15.41	15.31	14.61	13.16	14.31	15.39	14.93	14.57	14.22	14.81	13.72	14.33	14.38	14.01	13.66	14.02	17.88	10.53
Fe_2O_3	2.65	2.11	0.71	0.71	0.8	1.82	1.21	2.50	1.55	1.72	1.99	1.4	1.67	1.95	1.76	1.83	1.85	1.14	2.34
FeO	-	-	-	-	-	-	-	-	-	-	-	-	-	-	-	-	-	-	-
MnO	0.04	0.03	0.02	0.01	-	0.02	-	0.02	0.01	0.02	0.03	0.03	0.02	0.04	0.04	0.04	0.04	0.03	0.01
MgO	0.66	0.42	0.28	-	0.09	0.86	0.65	0.42	0.09	0.17	0.52	0.74	0.38	0.13	0.08	0.08	0.1	-	0.3
CaO	2.60	2.06	2.49	0.95	0.83	2.07	3.53	2.08	1.32	0.48	1.05	1.55	1.1	1.14	1.14	1.25	1.18	1.22	0.47
Na_2O	6.19	5.37	5.64	5.1	7.72	5.81	6.63	6.49	4.45	3.97	4.23	4.67	4.33	4.19	3.96	4.3	4.15	6.19	3.51
K_2O	1.32	2.43	1.47	3.87	0.8	0.84	0.38	1.59	4.37	5.38	4.29	3.84	4.47	4.16	4.45	3.5	4.04	4.49	4.19
P_2O_5	0.12	0.08	0.07	0.09	0.03	0.08	0.02	0.07	0.05	0.05	0.14	0.05	0.07	0.12	0.08	0.06	0.11	0.02	0.03
LOI	0.54	0.38	0.6	0.4	0.42	0.77	0.5	0.52	0.44	0.72	0.57	0.27	0.5	0.81	0.7	0.73	0.75	0.51	0.24
Total	100.53	100.33	100.43	100.35	99.27	100.04	99.83		100.35	100.19	100.4	99.72		100.13	100.27	99.07		100.48	99.88
Trace elements in ppm																			
Rb	73	76	40	69	20	44	25	50	138	175	137	121	142	324	349	310	328	162	90
Sr	579	488	529	393	124	194	177	355	197	115	246	145	176	139	121	121	127	211	24
Y	13	13	7	6	6	5	3	8	9	13	20	5	12	48	41	30	40	10	41
Zr	179	109	113	33	24	82	23	80	99	157	215	22	123	147	139	122	136	98	244
Nb	8	7	6	3	6	9	4	6	6	7	10	5	7	20	21	20	20	5	19
Co	11	10	12	12	2	4	4	8	9	9	11	4	8	9	9	11	10	11	4
Ni	9	9	9	9	10	11	8	9	9	9	14	13	11	9	9	9	9	9	9
Cu	2	2	2	2	8	8	27	7	2	2	5	31	10	2	2	2	2	2	7
Zn	44	35	33	12	7	21	10	23	17	23	32	9	20	32	29	33	31	16	46
V	30	21	19	15	9	6	6	15	22	18	21	11	18	15	15	15	15	19	5
Cr	11	9	9	9	28	16	24	15	9	9	29	32	20	9	9	9	9	10	11
Ba	239	559	557	1695	127	143	224	506	593	1173	904	1056	932	542	515	398	485	720	512
Rare Earth Elements in ppm																			
La	31.6	25.1	25.3	-	-	-	-		61.5	26.8	45.9	-		-	17.8	26.5		24.7	-
Ce	60.3	44.3	48.1	-	-	-	-		120	50.7	99.6	-		-	45.3	59.2		48.1	-
Pr	6.13	4.93	4.88	-	-	-	-		12.2	5.31	10.5	-		-	5.16	6.95		4.4	-
Nd	21.1	17.5	16.8	-	-	-	-		39	17.6	36.3	-		-	20	26.8		14.1	-
Sm	3.19	2.78	2.38	-	-	-	-		3.95	2.33	5.93	-		-	4.35	5.97		1.93	-
Eu	0.76	0.67	0.68	-	-	-	-		0.77	0.48	0.67	-		-	0.55	0.68		0.38	-
Gd	2.25	2.18	1.61	-	-	-	-		1.97	1.6	4.44	-		-	4.12	4.96		1.28	-
Tb	0.31	0.29	0.2	-	-	-	-		0.2	0.2	0.6	-		-	0.67	0.59		0.16	-
Dy	1.68	1.54	0.93	-	-	-	-		0.84	1.08	3.07	-		-	3.96	2.84		0.73	-
Ho	0.33	0.29	0.16	-	-	-	-		0.14	0.23	0.55	-		-	0.77	0.53		0.13	-
Er	0.86	0.8	0.39	-	-	-	-		0.38	0.66	1.41	-		-	2.13	1.65		0.35	-
Tm	0.1	0.11	0.05	-	-	-	-		0.06	0.1	0.2	-		-	0.32	0.3		0.05	-
Yb	0.53	0.62	0.33	-	-	-	-		0.38	0.66	1.28	-		-	2.09	2.35		0.37	-
Lu	0.07	0.09	0.05	-	-	-	-		0.06	0.11	0.2	-		-	0.3	0.39		0.06	-
CIPW Norms																			
Q	21.15	25.48	27.51	27.93	27.35	30.13	23.85		27.21	27.79	28	27.13		29.68	30.29	32.05		12.57	39.6
C	0.27	0.39	0.08	0.51	-	0.27	-		0.23	1.11	1.63	-		1.2	1.19	0.68		0.66	-
Or	7.82	14.39	8.72	22.9	4.79	5.01	2.26		25.88	32.01	25.44	22.84		24.79	24.58	21.06		26.57	24.9
Ab	52.51	45.54	47.88	43.21	63.99	49.6	56.53		37.73	33.82	35.91	39.78		35.75	35.44	37.05		52.44	29.86
An	12.15	9.72	11.94	4.13	-	9.83	11.18		6.24	2.07	4.31	5.15		4.91	4.87	5.92		5.93	0.59
Di	-	-	-	-	3.44	-	5.21		-	-	-	1.86		-	-	-		-	1.33
DiWo	-	-	-	-	1.66	-	2.64		-	-	-	0.94		-	-	-		-	0.65
DiEn	-	-	-	-	0.31	-	1.37		-	-	-	0.48		-	-	-		-	0.16
DiFs	-	-	-	-	1.47	-	1.2		-	-	-	0.44		-	-	-		-	0.53
Hy	4.55	3.2	2.7	0.81	-	4.19	0.48		1.8	2.26	3.16	2.61		2.39	2.37	2.15		1.28	2.58
HyEn	1.64	1.04	0.7	-	-	2.15	0.25		0.22	0.42	1.29	1.37		0.33	0.32	0.2		-	0.59
HyFs	2.91	2.15	2	0.81	-	2.03	0.22		1.58	1.84	1.87	1.25		2.07	2.05	1.95		1.28	1.99
Mt	0.53	0.53	0.49	0.13	-	0.44	0.28		0.39	0.43	0.52	0.33		0.49	0.49	0.47		0.28	0.57
Ap	0.26	0.18	0.15	0.2	0.07	0.18	0.04		0.11	0.11	0.31	0.11		0.26	0.26	0.13		0.04	0.07
Il	0.72	0.55	0.51	0.15	0.08	0.33	0.13		0.4	0.38	0.69	0.15		0.48	0.47	0.46		0.21	0.48
Ac	-	-	-	-	0.37	-	-		-	-	-	-		-	-	-		-	-
P	64.66	55.27	59.83	47.34	64	59.45	67.72		43.98	35.89	40.23	44.94		40.67	40.32	42.98		58.38	30.46
Q	21.15	25.41	27.45	27.93	27.38	30.09	23.83		27.16	27.74	27.92	27.1		29.62	30.23	31.99		12.54	39.53
A	7.82	14.4	8.72	22.9	4.79	5.01	2.26		25.88	32.01	25.44	22.85		24.8	24.58	21.07		26.57	24.9
Colour Ind	5.8	4.28	3.7	1.09	3.02	4.95	6.1		2.59	3.07	4.37	4.96		3.36	3.33	3.09		1.77	4.96
Diff.Index	81.48	85.42	84.11	94.04	96.13	84.74	82.65		90.81	93.61	89.34	89.75		90.23	90.31	90.17		91.58	94.36

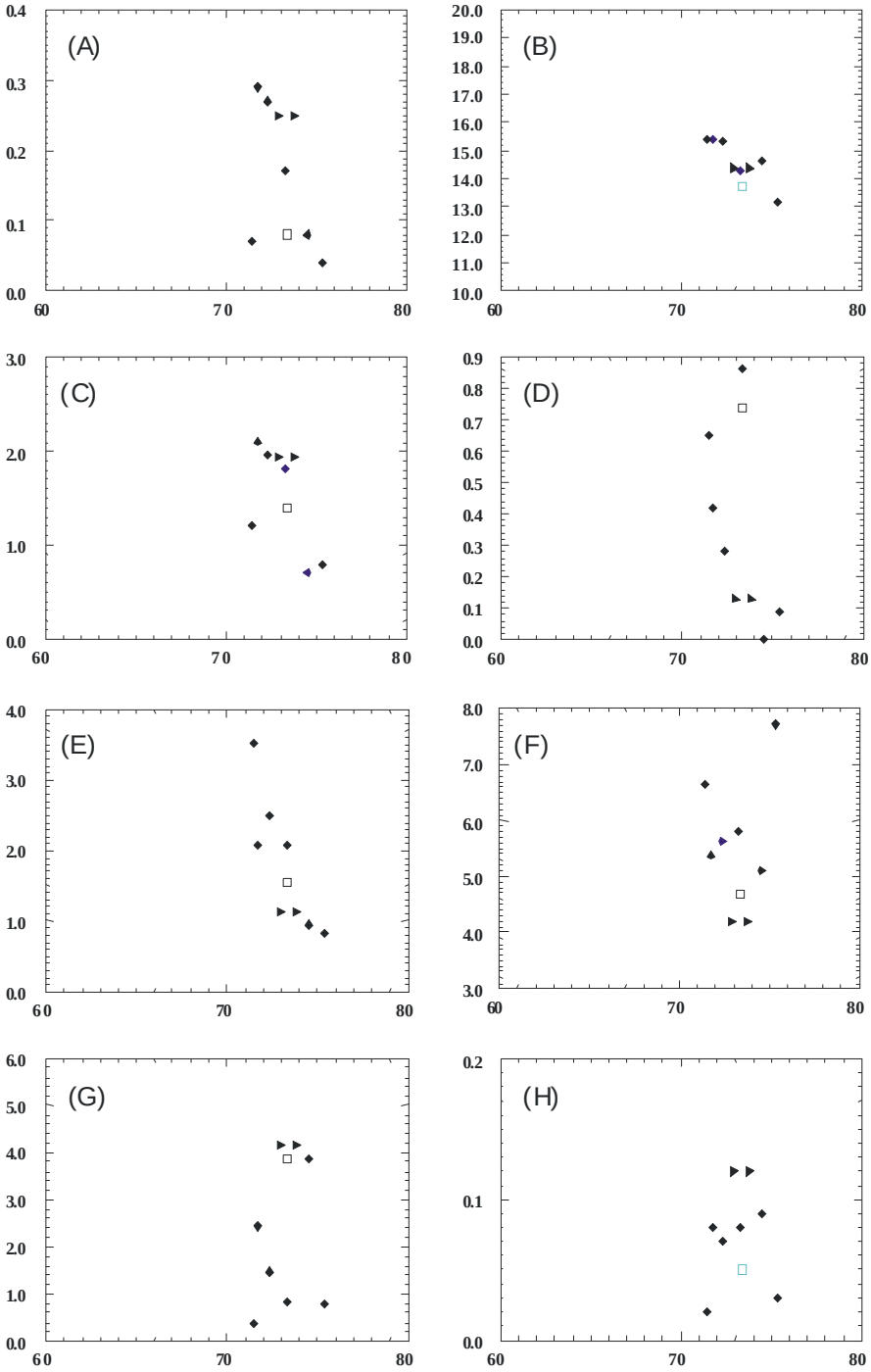

Figure 3. *Harker-type major-element variation diagrams for the Makoppa Dome granitoid rocks (Figure 1 and Table 1). Symbols depict Vaalpenskraal trondhjemitic gneisses (solid diamonds); Makoppa granodiorites/adamellites (half-filled squares); Rietkuil granodiorites (solid triangles); Aplitic dyke sample MK4 (open diamond); and Gaberone Granite sample MK27 (open square).*

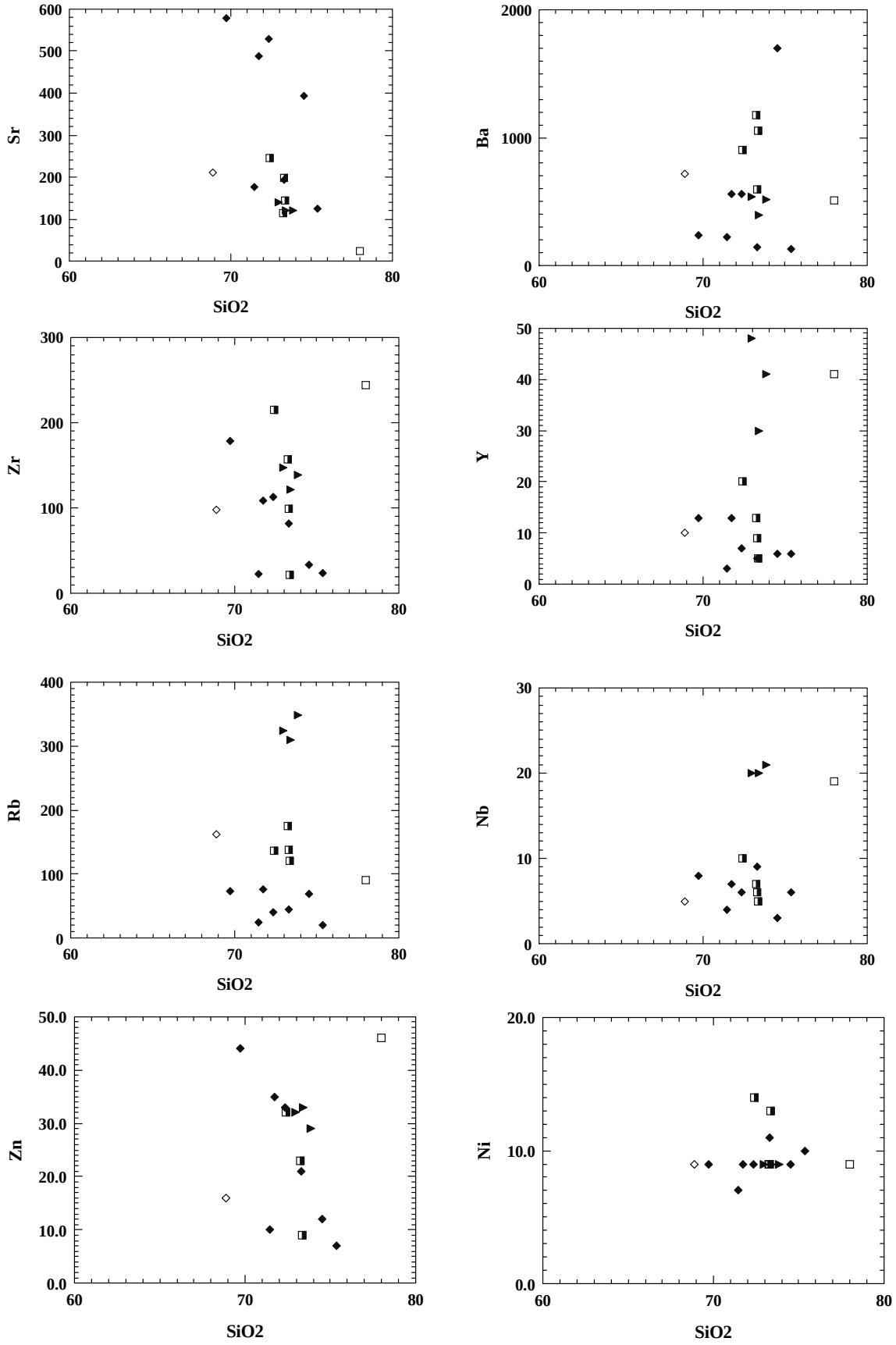

Figure 4. *Plots of SiO_2 (wt%) versus trace elements (ppm) of Sr, Ba, Zr, Y, Rb, Nb, Zn and Ni for the Makoppa granitoid rocks listed in Table 1 (symbols as in Figure 3).*

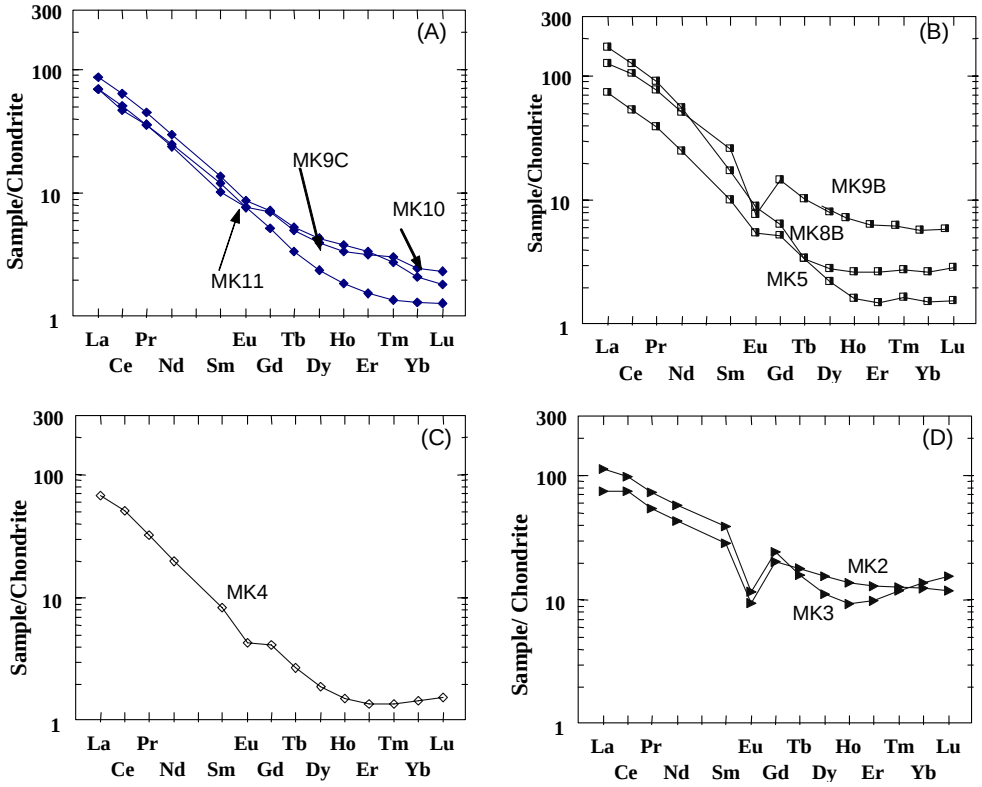

Figure 5. *Chondrite-normalized rare-earth element plots for rocks of the Makoppa Dome. (REE data from Table 1; symbols as in Figs. 3 and 4). (A). Vaalpenskraal trondhjemitic gneisses; (B). Makoppa granodiorites/adamellites; (C). Aplitic dyke sample MK4; and (D). Rietkuil granodiorites.*

between the light and heavy REEs and negligible or very slight Eu anomalies. In this respect the Vaalpenskraal trondhjemites show similar REE patterns to those reported for trondhjemites elsewhere on the Kaapvaal Craton including those of the Johannesburg Dome (Anhaeusser, 1999) as well as Swaziland, southern Mpumalanga and KwaZulu-Natal (Hunter *et al*., 1992).

Makoppa-type granodiorites/adamellites

As implied by the name the Makoppa-type granodiorites/adamellites are best exposed in the vicinity of the Makoppa settlement (Figure 1). Their presence is, however, believed to be far more extensive throughout the dome as is suggested by the presence of K-rich granitoid phases (including homogeneous granodiorites and pegmatites) wherever exposures enable observations to be made. Localities for sampling this granite-type are rare and suitable material for geochemical and isotopic study could only be obtained from the Crocodile River northwest of Makoppa and along the Marico River in the Welgewaagd area (Figure 1).

Near Makoppa, platform exposures in the river downstream of the bridge and weir (Figure 2 C, D) comprise homogeneous, reddish, coarse-grained, porphyritic granodioritic to adamellitic

rocks intruded by late-stage, red-coloured, fine-grained aplitic dykes and coarse-grained pegmatite (Figure 2 C, E). Petrologically the coarse-textured granodiorite/adamellite contains prominent amounts of K-feldspar (microcline, perthite) and quartz, with lesser biotite, albitic plagioclase, epidote, muscovite, sericite, ilmenite and leucoxene. The plagioclase shows partial sericitic alteration and vermicular quartz (myrmekite) replaces K-feldspar. The pegmatites are very coarse grained, consisting mainly of microcline, quartz and biotite. In places microcline crystals up to 13 cm in size in a white quartz matrix were noted.

Very fine-grained, homogeneous, reddish aplitic dykes (usually less than 50cm in width) intrude the porphyritic granitoids, and in places show a weak foliation parallel to the dyke margins suggesting some mineral orientation during emplacement. The aplitic dykes consist of finely crystalline quartz, feldspar (plagioclase and microcline) and epidote, together with accessory amounts of biotite, magnetite, apatite and sericite.

The Makoppa-type granitoids differ geochemically from the Vaalpenskraal trondhjemites in being more K_2O and Rb enriched (Table 1, columns 9-12). An average major element composition (column 12) shows an increase in K_2O, Rb and Zr and a corresponding decrease in Na_2O, CaO, Sr and Ba, relative to average trondhjemite (column 8). Major and trace element data is portrayed diagrammatically in Figures 3 and 4 together with values obtained from the two other granitoid varieties on the dome. Apart from some clustering of the Al_2O_3, Fe_2O_3 , CaO, Na_2O and K_2O major element data and the Sr, Ba, Y, Rb and Nb trace element data there is no clearly consistent pattern to the chemical behaviour of these rocks.

REE data for three samples of Makoppa-type granitoids are listed in Table 1 (columns 9-11) and are shown diagrammatically in Figure 4B. One sample (MK9B) displays a negative Eu anomaly, LREE enrichment and a moderate HREE pattern, whereas samples MK8 and MK5 show LREE enrichment, weak Eu anomalies and depleted HREEs. Sample MK 5 has a similar REE pattern to that of the aplitic dyke shown in Figure 5C suggesting that the aplitic dykes may represent late-stage anatectic melts of the Makoppa-type granitoids. The aplitic dyke (MK4) does, however, show SiO_2, TiO_2, Fe_2O_3, Zr and Ba depletion and Al_2O_3, CaO, Na_2O, Rb and Sr enrichment relative to the average Makoppa-type granitoids. The resultant chemical variations may reflect changes in composition of the melt resulting from pressure-quenching, and rapid crystallization (with consequent late-stage saturation in H_2O) that has been used to explain the common aplite-pegmatite association (Clarke, 1992).

Rietkuil-type granodiorites

What are believed to be the latest in the series of granitoid rocks developed on the Makoppa Dome are exposures of homogeneous, grey to pink, medium-grained granodiorites which are best exposed in the Rietkuil area on the eastern side of the dome, roughly midway between Thabazimbi and Sentrum (Figure 1). The mapping of Jansen *et al.* (1974) suggests that this granitoid variety may be widespread across the northeastern segment of the dome, but material most suitable for study was found among the tor-like outcrops on the farm Rietkuil 101KQ (Figure 2 F).

The Rietkuil-type granodiorites consist mainly of quartz, microcline and sericitized albitic plagioclase, together with subordinate biotite, chlorite, muscovite, epidote, sphene and magnetite. Also developed in places are some large K-feldspar megacrysts (some up to 2cm by 1cm in size) poikilitically enclosing crystals of quartz and plagioclase, and myrmekite,

which is an intergrowth of vermicular quartz in a sodic feldspar host, believed by Castle and Lindsley (1993) to have originated as a result of subsolidus unmixing of K-bearing plagioclase in a ternary feldspar system open to excess Si.

Table 1 (columns 14-17) lists three analyses and an average composition of Rietkuil-type granodiorite. Geochemically there is little to distinguish between the major element compositions of the Rietkuil and the Makoppa-type granodiorites, but trace element variations are more apparent (*cf*. columns 13 and 17). When compared with the Makoppa-type average there is a slight increase in SiO_2, TiO_2, Fe_2O_3, CaO and P_2O_5 and depletion in Al_2O_3, MgO, Na_2O and K_2O. Trace elements show enrichment in Rb, Y, Zr, Nb and V and Ba contents and depletion in Sr, Cr, and Ba. The close correspondence of the major elements can be seen diagrammatically in binary variation plots (Figure 3). By contrast the trace elements display clear separation, particularly with Ba, Y, Rb and Nb (Figure 3).

REE data for Rietkuil-type granodiorites is plotted in Figure 5D and reflects an overall flatter pattern than any of the other granitoid varieties so far described. There is a relative enrichment in LREE, moderate HREE abundances and a conspicuous negative Eu anomaly. The REEs help to quantify geochemically the distinctions already alluded to and which involve, in particular, very definitive field characteristics. It might be argued that the Reitkuil granitoids are similar to some phases of the Makoppa-type granitoids (*cf*. REE patterns of Rietkuil samples MK2 and MK3 with Makoppa sample MK9B; Figure 5B,D). Field criteria as well as trace element data show, however, that the Rietkuil samples are enriched in SiO_2, CaO, Rb, Y and Nb, and depleted in TiO_2, Al_2O_3, Fe_2O_3, MgO, P_2O_5, Sr, Zr, Ni, V, and Ba, relative to sample MK 9B of the Makoppa-type (Table 1). Thus, it is maintained that on field characteristics, as well as petrological and geochemical grounds, the three Makoppa granitoid types identified are distinctive. Additional support for this three-fold separation of the Makoppa granitoid rocks is provided in the geochronological section of this paper.

Geochemical discrimination

In a manner similar to that used to categorize granitic rocks on the Johannesburg Dome (Anhaeusser, 1999), the Makoppa geochemical data was subjected to discrimination procedures aimed at extracting genetic information and determining likely tectono-magmatic settings for the evolution of the Archaean basement rocks on the northwestern edge of the Kaapvaal Craton. Whilst, arguably, there may be shortcomings with the use of geochemical discrimination methods as petrogenetic or tectonic environmental indicators (Clarke, 1992) there appears to be increasing acceptance that they do contribute information relevant to geological processes and they enable comparisons to be made between modern and ancient geological terranes (Cassidy *et al*., 1991; Witt and Davy, 1997).

The Makoppa geochemical data has been plotted in a number of discrimination diagrams (Figure 6). Modal proportions of quartz, alkali feldspar and plagioclase (QAP) derived from CIPW normative mineralogy listed in Table 1, demonstrates that the Makoppa granitoids fall mainly into the fields of tonalite, granodiorite and monzogranite (Figure 6A, after Streckeisen, 1976). The term tonalite is, however, deemed inappropriate for the Vaalpenskraal granitoids and preference is given to the term trondhjemite for these rocks (see the IUGS definition of trondhjemite as leucotonalite - Barker, 1979).

The Makoppa granitoids are alumina-oversaturated (i.e., peraluminous, Figure 6E), the excess

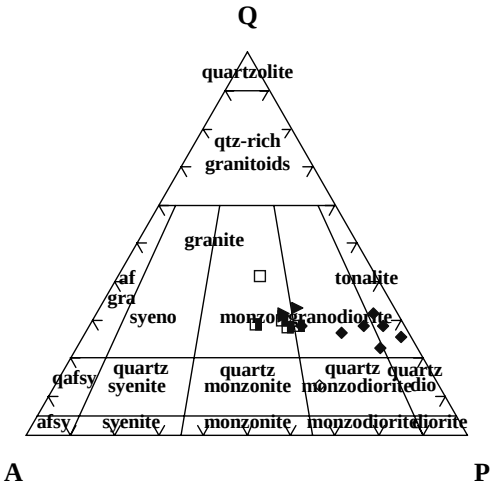
Q
quartzolite
qtz-rich
granitoids
granite
af
gra
syeno
tonalite
monzogranodiorite
qafsy
quartz
syenite
quartz
monzonite
quartz
monzodiorite
quartz
dio
afsy
syenite
monzonite
monzodiorite
diorite
A
P

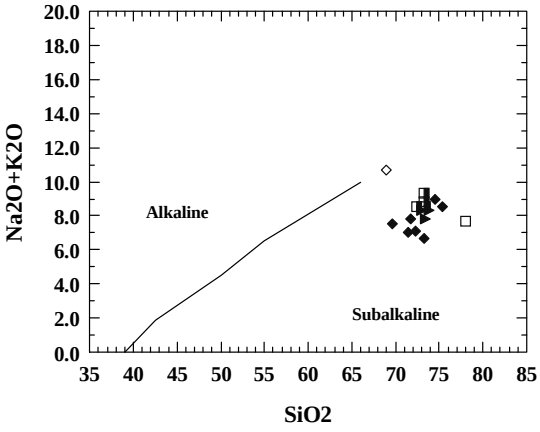
Na2O+K2O
Alkaline
Subalkaline
SiO2

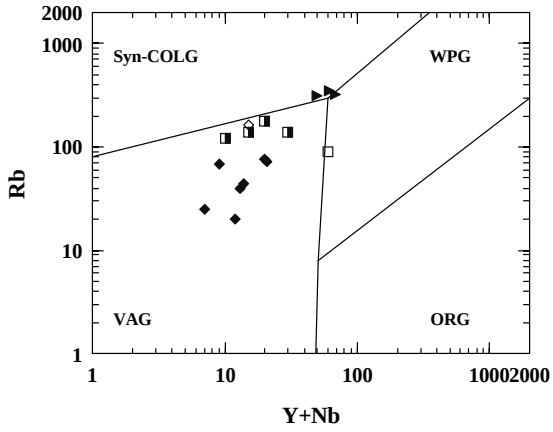
Rb
Syn-COLG
WPG
VAG
ORG
Y+Nb

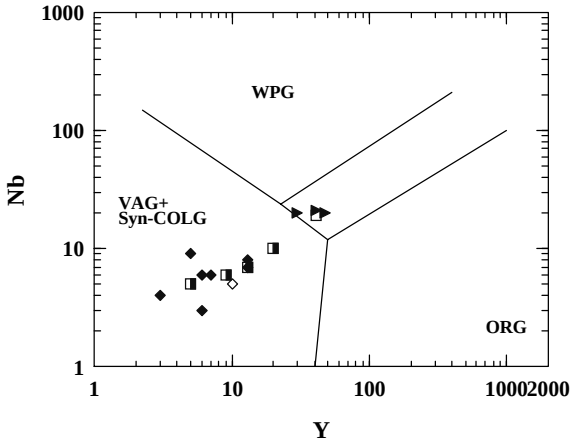
Nb
WPG
VAG+
Syn-COLG
ORG
Y

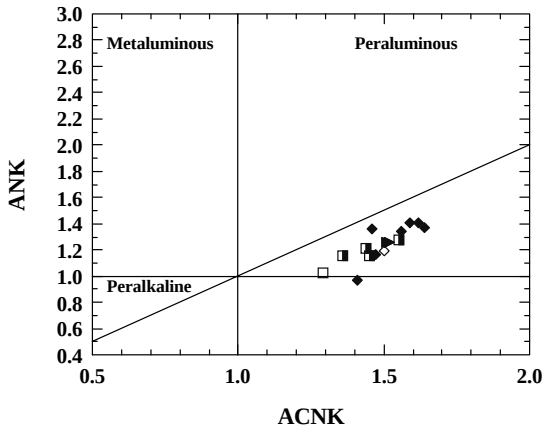
ANK
Metaluminous
Peraluminous
Peralkaline
ACNK

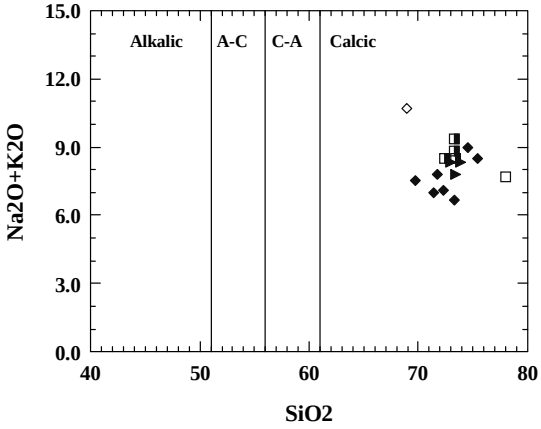
Na2O+K2O
Alkalic
A-C
C-A
Calcic
SiO2

Figure 6. (*A). QAP classification diagram of the granitoid rock suite after Streckeisen (1976). The Vaalpenskraal-type trondhjemitic gneisses (leucotonalites) plot in the tonalite and granodiorite fields, with the Makoppa and Rietkuil granitoids straddling the granodiorite-monzonite (adamellite) field with approximately equal proportions of plagioclase and alkali feldspar. The aplite dyke (sample MK4) plots in the quartz-monzodiorite field and the Gaborone Granite (sample MK27) approximates granite sensu stricto. (B). Total alkalies-silica diagram showing fields of alkaline and subalkaline rock suites. The line separating the two fields (after the 15 164 sample database of Le Bas et al., 1992), also separates nepheline-normative rocks (left) from rocks having no normative nepheline (right). (C). Rb versus Y+Nb diagram (after Pearce et al., 1984) showing the clustering of the Makoppa geochemical data into the volcanic-arc granite (VAG) field, suggesting that these granitoid rocks were developed in a volcanic arc setting in a manner similar to that proposed for the Archaean granitoid rocks of the Johannesburg Dome (Anhaeusser, 1999). (D). Nb-Y discriminant diagram (after Pearce et al., 1984) showing the clustering of the Vaalpenskraal- and Makoppa-type granitoid data in the VAG-SynCOLG field of volcanic-arc related tectonic settings. Note, however, the positions of the Rietkuil and Gaborone Granite samples which plot inside or adjacent to the within-plate granite (WPG) field (cf. plot C), suggesting there may be a genetic link between these late granitoids. (E). ANK versus ACNK diagram (after Maniar and Piccoli, 1989), showing the clustering of the Makoppa granitoids in the alumina-saturated or peraluminous field. (F). Total alkalies versus SiO_2 diagram (alkali-lime index, after Peacock, 1931) showing the clustering of the Makoppa granitoid data in the calcic field (now largely designated 'calc-alkaline suite' rocks with relative enrichment in silica and alkalies and little enrichment in Fe). Symbols in all diagrams as in Figure 3.*

alumina probably being accommodated in Al-rich biotite and muscovite present in the rocks. The granitoids are also silica-saturated or silica-oversaturated subalkaline rocks (Figure 6B) lacking normative nepheline, and they cluster in the calcic field of the SiO_2 versus Na_2O + K_2O diagram (the alkali-lime index plot of Peacock, 1931- Figure 6F). In this regard they are similar to the tonalitic rocks of the Mesozoic Cordilleran batholiths, which tend to plot entirely in the calcic field (Frost *et al*., 2001). The features thus described are consistent with the Makoppa granitoids having been formed and emplaced in volcanic-arc (VAG) and volcanic-arc and/or syn-collisional (VAG+syn COLG) geotectonic settings (Figs. 6C,D). By contrast the Gaborone granite sample, included in this study for comparative purposes, plots in the within-plate granite field (WPG) of Figure 6C,D (see also Sibiya, 1988, p.74) suggesting that this Archaean rapakivi granite-anorthosite-rhyolite complex may represent a post-tectonic, anorogenic or A-type magmatic event. It should be noted too that the Rietkul granitoids, although distinctive in terms of their major and trace element characteristics (*cf*. columns 17 and 19, Table 1), appear to have some affinity with the Gaborone granitoids in terms of age similarities (see later) and with regard to their position close to WPG field in the trace element discrimination diagrams shown in Figure 6C and D.

GEOCHRONOLOGY

Analytical techniques

Mineral separates were prepared from 4-6kg rock samples in the Hugh Allsopp Laboratory, University of the Witwatersrand, Johannesburg. Rock samples were pulverized using a heavy-duty hydraulic rock splitter, jaw crusher and swing mill. Mineral separation involved the use of a Wilfley Table, heavy liquids (bromoform and methylene iodide) and a Frantz Isodynamic Separator.

U-Pb single zircon ID-TIMS technique

Isotope Dilution-Thermal Ionization Mass Spectrometer (ID-TIMS) analyses were performed at Memorial University of Newfoundland, Canada. Normal transmitted and reflected light microscopy as well as SEM back-scattered or cathodoluminescence imagery were used to determine the zircon internal structures prior to analysis. Handpicked zircons were abraded (Krogh, 1982) and then washed in dilute nitric acid and ultra-pure acetone. Single grains or small populations of zircons were then placed into 0.35 ml Teflon vials together with 30 µl HF and a mixed ^{205}Pb-^{235}U spike. Eight of these Teflon vials were then placed in a Parr Container for 2 days at 210^{o}C (Parrish, 1987). The samples were measured on a Finnigan MAT262 mass spectrometer equipped with an ion-counting secondary electron multiplier. A detailed account of the entire analytical technique is given by Dubé *et al*. (1996). The calculation of common Pb was made by subtracting blanks and then assuming that the remaining common Pb has an Archaean composition determined from the model of Stacey and Kramers (1975). Data were reduced using PbDat (Ludwig, 1993). Analytical uncertainties in Table 2 are listed at 2σ and age determinations were processed using Isoplot/Ex (Ludwig, 2000).

LAM-ICP-MS technique

The U-Pb method followed is that described by Kosler *et al.* (2002). Laser Ablation Microprobe-Inductively Coupled Plasma-Mass Spectrometry (LAM-ICP-MS) analyses were

Table 2: ID-TIMS U-Pb data

- ***Sample MK10***

Grain	Weight µg	U (ppm)	Pb* (ppm)	Th/ U	$^{206}Pb/^{204}Pb$	Pb_c pg	Radiogenic Ratios						Ages (in Ma)				Rho 6/8-7/5
							$^{206}Pb/^{238}U$	± %	$^{207}Pb/^{235}U$	± %	$^{207}Pb/^{206}Pb$	± %	$^{206}Pb/^{238}U$	$^{207}Pb/^{235}U$	$^{207}Pb/^{206}Pb$	±	
Zr 1	6	810	238	0.28	1787	5	0.2699	3.2	6.504	3.2	0.1747	0.24	1541	2046	2604	4	0.997
Zr 2	4	54	22	0.13	680	10	0.3992	4.0	8.880	4.0	0.1613	0.81	2166	2326	2470	14	0.980
Zr 3	6	381	96	0.30	1302	6	0.2356	0.9	5.076	0.9	0.1563	0.20	1364	1832	2416	3	0.974

- ***Sample MK-11***

Grain	Weight µg	U (ppm)	Pb* (ppm)	Th/ U	$^{206}Pb/^{204}Pb$	Pb_c pg	Radiogenic Ratios						Ages (in Ma)				Rho 6/8-7/5
							$^{206}Pb/^{238}U$	± %	$^{207}Pb/^{235}U$	± %	$^{207}Pb/^{206}Pb$	± %	$^{206}Pb/^{238}U$	$^{207}Pb/^{235}U$	$^{207}Pb/^{206}Pb$	±	
Zr1 Y_2, T	3	249	118	0.05	1976	11	0.4595	0.2	11.947	0.2	0.1886	0.09	2437	2600	2730	1	0.940
Zr2 Y_3, T	3	302	134	0.24	813	28	0.4024	0.3	10.581	0.3	0.1907	0.07	2179	2487	2748	1	0.971
Zr3 Y, T	1	429	232	0.25	1307	10	0.4935	0.2	13.229	0.2	0.1944	0.07	2586	2695	2780	1	0.955
Zr4 Y, D	1.5	362	142	0.34	127	103	0.3400	0.2	8.414	0.3	0.1796	0.20	1885	2277	2649	3	0.727
Zr5 Y_4, T	3	363	154	0.19	599	45	0.3874	0.4	10.211	0.4	0.1912	0.08	2111	2454	2753	1	0.981
Zr6 Y_3, D	2.5	1087	410	0.11	1410	43	0.3554	1.2	9.110	1.2	0.1859	0.06	1960	2349	2706	1	0.999
Zr7 P, T	4	143	69	0.14	745	22	0.4517	0.3	12.079	0.3	0.1940	0.08	2403	2611	2776	1	0.952
Zr8 P, T	12	257	138	0.12	4331	22	0.5054	0.7	13.880	0.7	0.1992	0.04	2637	2742	2820	1	0.998
Zr9 P, T	4	301	128	0.06	1161	27	0.4089	0.2	10.607	0.2	0.1881	0.05	2210	2489	2726	1	0.954
Zr10 P, T	4	301	144	0.06	2581	13	0.4581	0.2	11.888	0.2	0.1882	0.08	2431	2596	2727	1	0.940
Zr11 P, T	10	156	75	0.41	1029	39	0.4123	3.0	11.090	3.0	0.1951	0.06	2225	2531	2785	1	1.000
Zr12 P_4, T	8	131	60	0.17	389	76	0.4303	0.5	11.170	0.5	0.1883	0.10	2307	2537	2727	2	0.979
Zr13 P, T	15	239	104	0.22	846	106	0.3933	0.2	10.326	0.2	0.1904	0.06	2138	2464	2746	1	0.941
Zr14 P, T	13	132	64	0.20	1272	38	0.4482	0.2	11.856	0.2	0.1918	0.06	2387	2593	2758	1	0.963

- ***Sample MK5***

Grain	Weight µg	U (ppm)	Pb* (ppm)	Th/ U	$^{206}Pb/^{204}Pb$	Pb_c pg	Radiogenic Ratios						Ages (in Ma)				Rho 6/8-7/5
							$^{206}Pb/^{238}U$	± %	$^{207}Pb/^{235}U$	± %	$^{207}Pb/^{206}Pb$	± %	$^{206}Pb/^{238}U$	$^{207}Pb/^{235}U$	$^{207}Pb/^{206}Pb$	±	
Zr 1 P, T	14	27	18	0.45	4523	3	0.5645	0.4	16.157	0.3	0.2076	0.16	2885	2886	2887	3	0.907
Zr 2 P, T	7	49	33	0.52	2003	6	0.5539	0.6	15.756	0.5	0.2063	0.43	2841	2862	2877	7	0.828

Zr 3 P, T	5	30	20	0.53	511	11	0.5510	0.3	15.635	0.3	0.2058	0.17	2829	2855	2873	3	0.858
Zr 4 S, T	31	47	31	0.52	4796	11	0.5645	0.4	16.143	0.4	0.2071	0.06	2885	2885	2883	1	0.989
Zr 5 P, T	10	23	15	0.57	1818	4	0.5486	0.5	15.523	0.5	0.2052	0.12	2819	2848	2868	2	0.971
Zr 6 P, T	12	20	12	0.35	807	10	0.5559	0.6	15.828	0.5	0.2065	0.19	2850	2866	2878	3	0.878
Zr 7 P, T	12	17	12	0.72	467	16	0.5591	0.3	15.923	0.3	0.2066	0.31	2863	2872	2879	5	0.903
Zr 8 P, T	12	40	25	0.45	2907	5	0.5423	0.9	15.247	0.9	0.2039	0.17	2793	2831	2858	3	0.982
Zr 9 P_2, T	6	25	15	0.50	684	7	0.5316	4.2	14.712	4.2	0.2007	0.20	2748	2797	2832	3	0.999

- ***Sample MK2***

Grain	Weight µg	U (ppm)	Pb* (ppm)	Th/ U	$^{206}Pb/^{204}Pb$	Pb_c pg	Radiogenic Ratios $^{206}Pb/^{238}U$	± %	$^{207}Pb/^{235}U$	± %	$^{207}Pb/^{206}Pb$	± %	Ages (in Ma) $^{206}Pb/^{238}U$	$^{207}Pb/^{235}U$	$^{207}Pb/^{206}Pb$	±	Rho 6/8-7/5
Zr 1 P, D	6	56	29	0.32	1044	6	0.4595	0.2	11.869	0.3	0.1873	0.08	2438	2594	2719	1	0.955
Zr 2 P, D	6	140	40	0.14	858	11	0.2614	0.4	6.355	0.4	0.1763	0.19	1497	2026	2619	3	0.912
Zr 3 P, T	4	616	172	0.27	1559	24	0.2469	0.4	5.025	0.4	0.1476	0.07	1422	1823	2319	1	0.984
Zr 4 P, T	4	51	27	0.76	2131	3	0.4203	0.4	10.696	0.4	0.1846	0.14	2262	2497	2694	2	0.999
Zr 5 P, D	4	127	62	0.47	5985	2	0.4139	0.4	10.402	0.4	0.1823	0.11	2233	2472	2674	2	0.956
Zr 6 P, D	4	510	152	0.19	923	39	0.2733	0.4	6.025	0.4	0.1599	0.08	1158	1979	2454	1	0.979
Zr 7 P, D	4	102	53	0.48	618	19	0.4425	0.4	11.326	0.4	0.1857	0.15	2362	2550	2704	2	0.932
Zr 8 P, D	5	321	153	0.35	1734	6	0.2836	11	6.189	11	0.1583	0.81	1610	2003	2437	14	0.997

- ***Sample MK3***

Grain	Weight µg	U (ppm)	Pb* (ppm)	Th/ U	$^{206}Pb/^{204}Pb$	Pb_c pg	Radiogenic Ratios $^{206}Pb/^{238}U$	± %	$^{207}Pb/^{235}U$	± %	$^{207}Pb/^{206}Pb$	± %	Ages (in Ma) $^{206}Pb/^{238}U$	$^{207}Pb/^{235}U$	$^{207}Pb/^{206}Pb$	±	Rho 6/8-7/5
Zr 1 R, T	8	274	146	0.40	6127	10	0.4684	0.2	12.272	0.2	0.1900	0.06	2477	2625	2742	1	0.971
Zr 2 R, D	6	111	40	044	555	33	0.2966	0.5	7.566	0.7	0.1850	0.56	1674	2181	2698	9	0.639
Zr 3 R, T	6	188	61	0.29	943	21	0.2795	0.4	6.871	0.4	0.1783	0.15	1589	2095	2637	3	0.923
Zr 4 P, T	4	39	22	0.40	771	6	0.4939	0.4	13.104	0.3	0.1924	0.23	2587	2687	2763	4	0.851
Zr 5 P_3, T	8	89	40	0.38	1416	10	0.3868	0.2	9.618	0.2	0.1803	0.09	2108	2399	2656	1	0.918
Zr 6 P, T	4	116	52	0.39	1684	7	0.3861	0.6	9.562	0.6	0.1796	0.23	2105	2394	2649	2	0.986
Zr 7 P_2, T	4	111	53	0.36	1852	7	0.4236	0.4	10.809	0.3	0.1851	0.23	2277	2507	2699	4	0.867
Zr 8 P, T	3	1108	301	0.17	1344	31	0.2508	0.3	5.508	0.3	0.1592	0.07	1443	1902	2448	1	0.974

performed in the Department of Earth Sciences at Memorial University, using a VG PlasmaQuad 2 S+ coupled to an in-house custom-built Q switched Nd:YAG ultraviolet laser operating with a wavelength of 266 nm. Zircons were ablated using a laser repetition rate of 10Hz and a laser energy of 0.8 mJ/pulse. The laser beam was focussed 100 µm above the sample surface and reduced to a diameter of 10 to 20 µm by masking with a white Teflon® aperture. The sample cell was mounted on a computer-driven motorized stage on the microscope. The computer-driven stage was moved beneath the stationary laser to produce a rectangular pit of variable length, usually in the range of 20 to 40 µm, in order to match zircon crystal size. The depth of the pit varied from *c.* 10 to 50 µm depending on line/pit length and ablation time. Using He as a carrier gas, the ablated sample material was transported, via acid-washed plastic tubing, from the sample cell to the ICPMS. Data was acquired to allow measurement of the U/Pb and Pb-isotopic ratios in zircons, as well as the isotopic ratios in the Tl/Bi/Np tracer solution that was nebulized simultaneously with the laser-ablated solid sample. The tracer solution contained natural Tl ($^{205}Tl/^{203}Tl$=2.3871), ^{209}Bi and ^{237}Np at concentrations of approximately 10 ppb for each isotope. Typical time-resolved data acquisitions consisted of *c.* 60 sec measurements of the He gas blank and tracer solution signals just before the start of ablation. The U and Pb zircon ablation signals, together with the simultaneous Tl/Bi/Np solution signals, were acquired after a further 180 to 200 secs. The data were acquired in peak jumping-pulse counting mode with 1 point measured per peak using PQVision v. 4.30 software. In total 11 masses were measured, 201 (flyback), 203 (Tl), 204 (Pb), 205 (Tl), 206 (Pb), 207 (Pb), 209 (Bi), 237 (Np) and 238 (U) and oxides of Np ($^{237}Np^{16}O$ = 254) and U ($^{238}U^{16}O$ = 254) were monitored to correct for oxide formation. Quadrupole settling time was 1 ms for all masses and the dwell time was 8.3 ms for all masses except for mass 207 where it was 24.9 ms. Over the 240 seconds of measurement approximately 1600 data acquisition cycles (sweeps) were collected. Final ages and concordia diagrams were produced using the Isoplot/Ex macro (Ludwig, 2000) in conjunction with the LAMdate Excel spreadsheet program (Kosler *et al.,* 2002). All data are reported in Table 3.

Geochronological results

Vaalpenskaal-type trondhjemitic gneisses (samples MK10 and MK11)

Zircons extracted from sample MK10 were generally light pink to yellowish in colour, and fairly translucent. The shapes varied from elongated to more prismatic. Some grains were slightly rounded at the edges (Figure 7C). Cathodoluminescence imaging (Figure 7A-D) revealed complex internal structures for these zircons, with bright-zoned “core” and darker-zoned rims (Figure 7A, B). More rarely, the grains show good igneous zoning (Figure 7C, D). Attempts to date this sample using the ID-TIMS technique (Table 2 and Figure 8) resulted in very discordant and scattered zircons as shown in Figure 8. The LAM-ICP-MS technique was then chosen as it allows a more selective analytical approach of data collection. Twenty-nine single spots from 25 zircon grains were analyzed and data are reported in Table 3 and plotted on Figure 8. A weighted mean $^{207}Pb/^{206}Pb$ age calculated for the more than 90% concordant points (shaded ellipses on Figure 8) gives 3013 ± 11 Ma (MSWD = 1.02). An upper intercept age calculated for all these analyses plus spots 7.1 and 12.1 (Figure 8) gives a similar age of 3011 +30/-29 Ma (MSWD = 0.38). This date of *c.* 3010 Ma is regarded as the age for the emplacement of this trondhjemite in the region. Nine spots (Zr 01-1, 02-1, 04-2, 06-1, 06-2, 09-1, 11-1, 14-1 and 15-1) plot in a more discordant position (Figure 8). A group of 6 of these measured spots (Zr 01-1, 02-1, 06-1, 06-2, 09-1, and 15-1) gives an upper intercept age of 2629 ± 130 Ma (MSWD=0.90, Figure 8 inset), the remaining 3 spots plotting in an

Table 3: LAM-ICP-MS data

- ***Sample MK 10***

Grain. spot	Radiogenic Ratios						Ages (in Ma)				Conc. %
	$^{206}Pb/^{238}U$	±	$^{207}Pb/^{235}U$	±	$^{207}Pb/^{206}Pb$	±	$^{206}Pb/^{238}U$	$^{207}Pb/^{235}U$	$^{207}Pb/^{206}Pb$	± 1σ	
01 1 rim	0.3525	0.0204	7.652	0.4980	0.1574	0.0061	1946	2191	2428	66	80
02 1 core	0.3003	0.0135	6.259	0.4439	0.1493	0.0054	1693	2013	2338	62	72
03 1 core	0.5603	0.0328	16.333	1.0268	0.2272	0.0157	2868	2897	3032	111	95
03 2 core	0.5822	0.0447	18.760	1.5500	0.2257	0.0126	2958	3030	3022	90	98
04 1 core	0.4422	0.0302	13.648	0.9820	0.2239	0.0152	2360	2726	3009	109	78
04 2 rim	0.3348	0.0114	8.123	0.3702	0.1760	0.0042	1862	2245	2615	39	71
05 1 rim	0.5952	0.0170	18.341	0.8181	0.2235	0.0188	3011	3008	3006	135	100
05 2 core	0.4258	0.0211	13.302	0.8153	0.2266	0.0035	2287	2701	3028	25	76
06 1 core	0.2584	0.0145	4.921	0.3570	0.1381	0.0045	1482	1806	2204	57	67
06 1 core	0.3368	0.0157	6.890	0.4552	0.1483	0.0054	1871	2097	2327	63	80
07 1 core	0.2531	0.0138	7.541	0.3788	0.2161	0.0086	1454	2178	2952	64	49
08 1 core	0.5117	0.0189	16.358	0.7840	0.2286	0.0079	2664	2898	3042	55	88
09 1 core	0.3107	0.0220	6.267	0.5973	0.1463	0.0046	1744	2014	2303	54	76
10 1 rim	0.5697	0.0175	17.599	0.6035	0.2242	0.0042	2907	2968	3011	30	97
11 1 core	0.1886	0.0183	4.390	0.6713	0.1688	0.0141	1114	1710	2546	140	44
12 1 core	0.2423	0.0135	7.582	0.4979	0.2269	0.0087	1399	2183	3030	62	46
13 1 rim	0.5531	0.0181	17.182	0.5077	0.2253	0.0045	2838	2945	3019	32	94
14 1 core	0.3363	0.0194	8.230	0.6499	0.1736	0.0060	1869	2257	2592	58	72
15 1 rim	0.4413	0.0238	10.595	0.6444	0.1741	0.0047	2356	2488	2598	45	91
16 1 core	0.5275	0.0238	16.241	0.6638	0.2233	0.0045	2731	2891	3005	32	91
17 1 core	0.4969	0.0345	16.043	1.1545	0.2342	0.0125	2600	2879	3081	86	84
18 1 core	0.4659	0.0248	14.585	0.7926	0.2270	0.0065	2466	2789	3031	46	81
19 1 core	0.5198	0.0416	16.719	1.3932	0.2333	0.0190	2698	2919	3075	130	88
20 1 core	0.5904	0.0299	18.166	0.7761	0.2232	0.0114	2991	2999	3004	82	100
21 1 core	0.5247	0.0302	15.778	1.2417	0.2181	0.0124	2719	2863	2967	92	92
22 1 core	0.5173	0.0376	15.077	1.1492	0.2114	0.0112	2688	2820	2916	86	92
23 1 core	0.4612	0.0237	14.411	0.8582	0.2266	0.0076	2445	2777	3028	54	81
24 1 core	0.5470	0.0212	16.586	0.6473	0.2199	0.0044	2813	2911	2980	32	94
25 1 core	0.4207	0.0242	12.894	0.6891	0.2223	0.0087	2263	2672	2998	63	76

- ***Sample MK11:***

Grain. spot	Radiogenic Ratios						Ages (in Ma)				Conc. %
	$^{206}Pb/^{238}U$	±	$^{207}Pb/^{235}U$	±	$^{207}Pb/^{206}Pb$	±	$^{206}Pb/^{238}U$	$^{207}Pb/^{235}U$	$^{207}Pb/^{206}Pb$	± 1σ	
01-1 rim	0.559	0.0193	15.931	0.5212	0.2094	0.0023	2862	2873	2901	18	99
01-2 core	0.387	0.0204	11.289	0.5682	0.2168	0.0037	2107	2547	2957	28	71
02-1 rim	0.391	0.0283	11.649	0.7192	0.2139	0.0082	2127	2577	2935	62	72
02-2 core	0.552	0.0128	17.114	0.3398	0.2420	0.0109	2834	2941	3133	72	90
03-1 rim	0.495	0.0291	13.358	0.8595	0.1971	0.0029	2593	2705	2802	24	92
04-1 rim	0.518	0.0170	14.395	0.4809	0.2033	0.0024	2691	2776	2853	19	94
05-1 rim	0.501	0.0135	13.567	0.4206	0.1995	0.0021	2618	2720	2822	17	93
07-1 core	0.399	0.0155	11.784	0.4653	0.2155	0.0040	2165	2587	2947	30	73
08-1 core	0.525	0.0199	16.605	0.5885	0.2288	0.0051	2721	2912	3044	35	89
09-1 core	0.524	0.0135	15.931	0.3827	0.2226	0.0039	2716	2873	3000	28	91
10-1 rim	0.488	0.0135	13.775	0.3830	0.2056	0.0022	2561	2734	2871	17	89

- ***Sample MK2:***

Grain. spot	Radiogenic Ratios						Ages (in Ma)				Conc. %
	$^{206}Pb/^{238}U$	±	$^{207}Pb/^{235}U$	±	$^{207}Pb/^{206}Pb$	±	$^{206}Pb/^{238}U$	$^{207}Pb/^{235}U$	$^{207}Pb/^{206}Pb$	± 1σ	
01-1 core	0.522	0.0171	14.170	0.604	0.1971	0.0059	2706	2761	2802	49	97
01-2 rim	0.453	0.0293	10.826	0.962	0.1793	0.0056	2508	2406	2647	52	91
01-3 rim	0.445	0.0138	11.096	0.351	0.1846	0.0021	2531	2744	2695	18	88
02-1 core	0.506	0.0237	13.923	0.612	0.2008	0.0082	2639	2745	2833	67	93
02-2 rim	0.200	0.0099	3.442	0.212	0.1252	0.0034	1514	1174	2032	48	58

03-1 core	0.308	0.0219	7.757	0.601	0.1784	0.0062	1732	2203	2638	58	66
04-1 core	0.547	0.0209	14.875	0.785	0.1972	0.0093	2813	2807	2804	77	100
05-1 core	0.203	0.0179	3.010	0.303	0.1085	0.0121	1433	1190	1775	204	67
06-1 rim	0.155	0.0144	1.851	0.217	0.0901	0.0048	1064	929	1482	65	65
06-2 rim	0.156	0.0128	1.932	0.220	0.0893	0.0054	1092	936	1410	66	66
07-1 core	0.200	0.0107	3.682	0.234	0.1372	0.0038	1567	1176	2193	48	54
08-1 rim	0.496	0.0488	12.970	1.537	0.2002	0.0127	2678	2596	2828	104	92
09-1 rim	0.490	0.0273	13.167	0.789	0.1963	0.0038	2692	2570	2796	32	92
10-1 core	0.387	0.0245	9.689	0.637	0.1934	0.0044	2406	2107	2771	37	76
11-1 core	0.178	0.0102	2.755	0.295	0.1161	0.0074	1343	1057	1898	114	56
12-1 rim	0.278	0.0225	5.917	0.704	0.1602	0.0042	1964	1581	2457	44	64
12-2 rim	0.215	0.0245	3.700	0.487	0.1273	0.0058	1571	1257	2062	80	61
13-1 core	0.513	0.0167	13.176	0.432	0.1883	0.0029	2692	2668	2727	25	98
13-2 core	0.520	0.0165	13.638	0.421	0.1935	0.0033	2725	2701	2773	28	97
14-1 core	0.546	0.0212	16.174	0.670	0.2162	0.0035	2887	2807	2952	26	95

Sample MK2 contd:

intermediate position between the two discordias. All these 6 spots were measured either on a zircon rim or in a zircon without a bright core. Although poorly constrained, this age of *c.* 2630 Ma is regarded as the minimum estimate for the metamorphic event that affected this sample and which led to the growing of rims and/or new zircon grains.

Sample MK11 presents small zircons mostly pink in colour, fairly translucent and elongated to prismatic in shapes (Figure 7E, F). As with sample MK10, some grains appear to be slightly rounded. Back-scattered pictures revealed the complex internal structures of these grains with the presence of cores showing igneous zoning surrounded by and/or embedded into more homogeneous rims (Figure 7E, F). Fourteen single zircon or small groups of zircons (maximum 4 grains) were analyzed using the ID-TIMS technique (Table 2). Reported in a concordia diagram, they plot in discordant to very discordant positions and do not define a simple, single group or trend, which may indicate the presence of more than one age population and probably the effects of more than one Pb-loss event. This is certainly the consequence of the complex internal structures of the grains. It is evident that the $^{207}Pb/^{206}Pb$ ages average around 2760 Ma. Eleven spots from 9 different grains were also analyzed by LAM-ICP-MS (Table 3). Plotted in a concordia diagram (Figure 9) the data, again, do not define a simple trend. Nevertheless, we interpret this complex age pattern as follows. Five analyses of cores (Zr 01-2, 02-2, 07-1, 08-1 and 09-1, Table 3) define an age of 3034 ± 64 Ma (MSWD=0.34). The analyses of the rims (Zr 01-1, 02-1, 03-1, 04-1, 05-1 and 10.1, Table 3) define an age of 2842 ± 35 Ma (MSWD=1.01). The 3034 ± 64 Ma age is within error of the age of 3011 ± 30 Ma found for sample MK10. It is consequently regarded as the best estimate for the emplacement age of sample MK11. The date of 2842 ± 35 Ma reflects the age of the metamorphic event that affected this sample.

Makoppa-type granodiorite/adamellite (sample MK5)

Zircons extracted from this sample were generally large grains, yellow to amber in colour, and translucent to metamict. Back-scattered imaging revealed relatively homogeneous grains with igneous zoning (Figure 7G, H) and fairly altered rims. Eight single grains and 1 group of 2 grains (Table 2) were analyzed using the ID-TIMS technique. They plot in a concordant to subconcordant position (Figure 10) and define an upper intercept age of 2886.4 +3/-2.3 Ma (MSWD=0.67) with a lower intercept age of 1280 +160/-140 Ma. This age of 2880 Ma is interpreted as the emplacement age of this granodiorite.

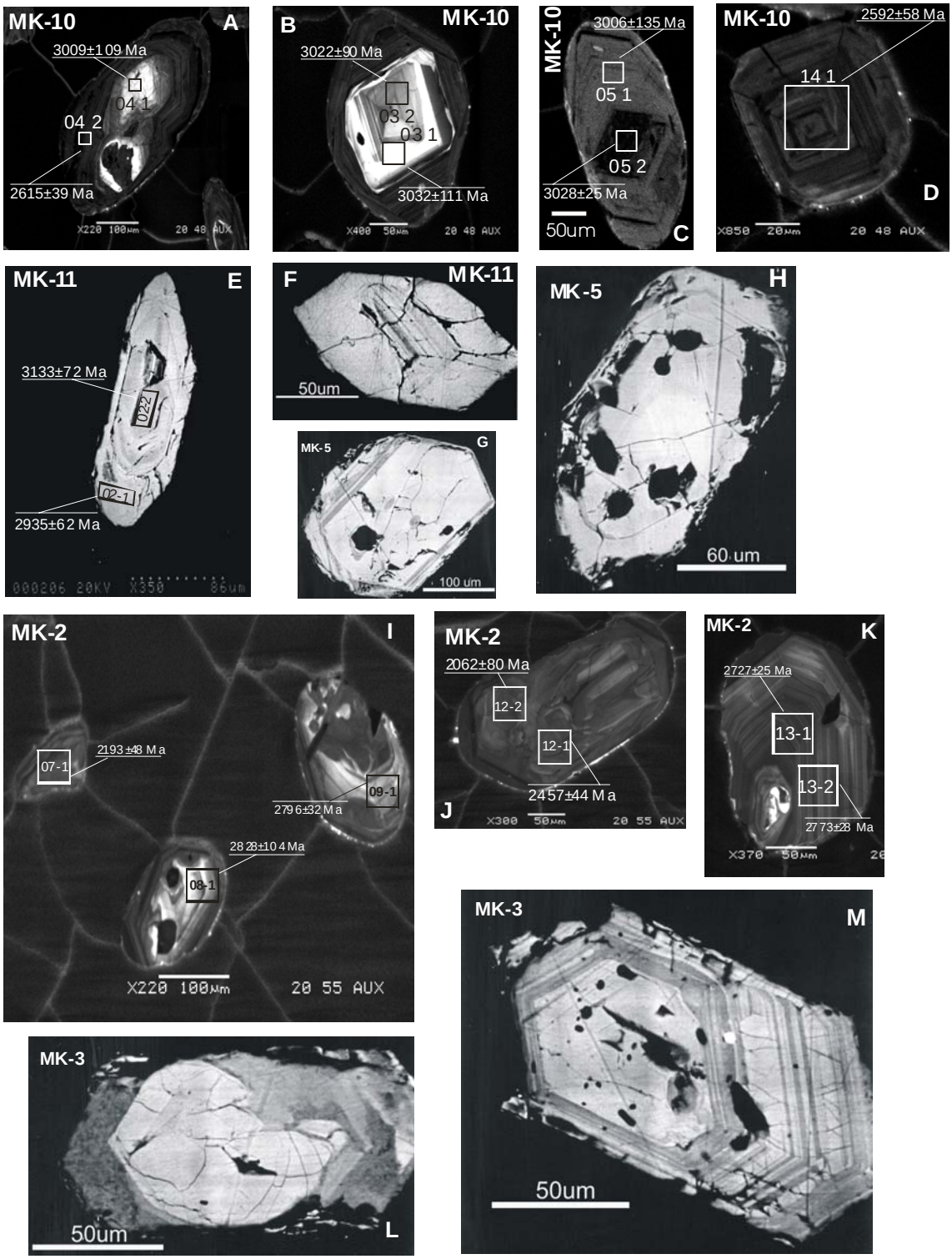

Figure 7. *Cathodoluminescence (CL) and back-scattered (BS) images for zircon crystals from samples MK10 (CL; A, B, C and D), MK11 (BS; E, F), MK5 (BS; G, H), MK2 (CL; I, J, K) and MK3 (BS; L, M).*

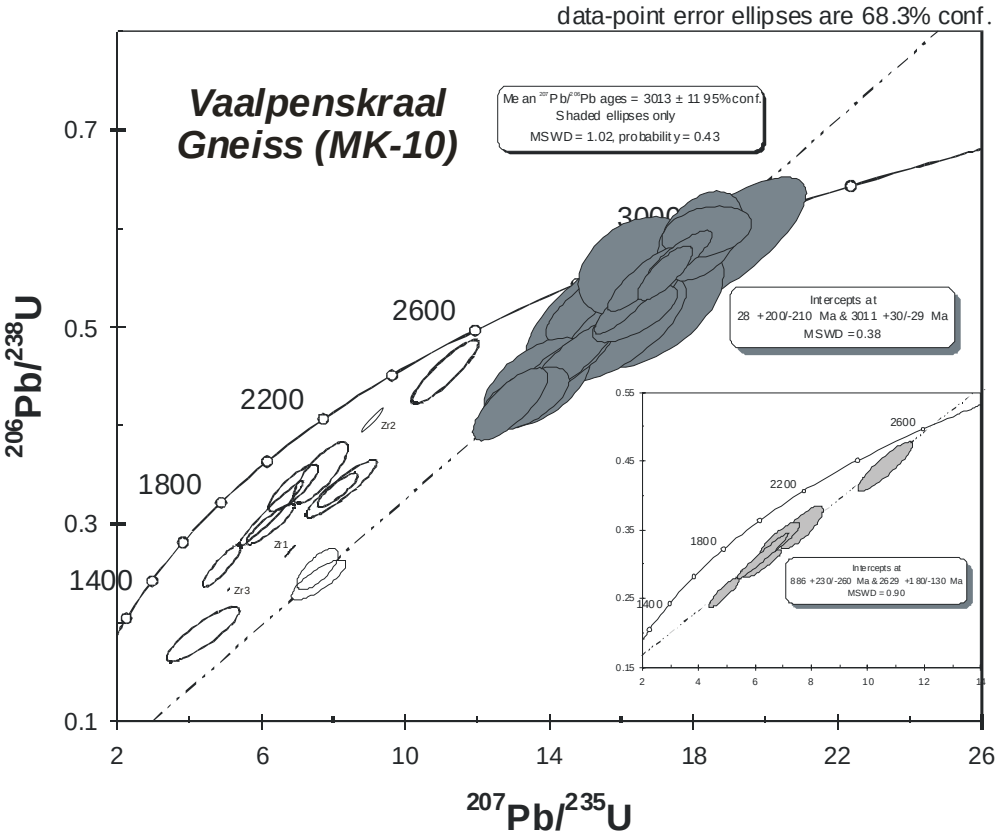

Figure 8. *Concordia diagram for Vaalpenskraal-type trondhjemitic gneiss sample MK10. Zr1, Zr2 and Zr3 correspond to the ID-TIMS measurements reported in Table 2.*

Rietkuil-type granodiorites (samples MK2 and MK3)

Sample MK2 presents mostly pink, translucent to metamict rounded zircons. Cathodoluminescence imaging shows the grains are characterized by complex internal structure (Figure 7 I, J) with ghost zoning in the cores and darker rims responsible for the rounded shape of the grains. Some zircons, however, display good igneous zoning (Figure 7 K) with darker rims still apparent. Eight single grains (Table 2) were dated using the ID-TIMS technique. Plotted in a concordia diagram (Figure 11A) they are all very discordant. A regression through all but zircon 2 yields an upper intercept age of 2777.3 ± 1.8 Ma (MSWD=0.098) with a lower intercept of 762 +5.7/-5.5 Ma. Because of the degree of discordance, this age of 2780 Ma can only be regarded as a minimum estimate for the emplacement of this granodiorite. In order to better constrain the age of emplacement, a LAM-ICP-MS dating was initiated. Twenty measurements were performed on 14 grains and the data are reported in Table 3 and plotted on Figure 11B. All the data except Zr 01-2, 03-1 and 14-1 yield an upper intercept age of 2777 ± 35 Ma (MSWD=0.76) and a lower intercept of 785 ± 60 Ma. The most concordant zircons define a weighted $^{207}Pb/^{206}Pb$ mean age of 2801 ± 24 Ma. This age of 2800 Ma is regarded as the best estimate for the emplacement of this granodiorite.

Zircons extracted from sample MK3 were pink to yellow in colour, very metamict, and with shapes varying from elongated to prismatic. Back-scattered imaging revealed zircons with either no zoning and a very corroded rim (Figure 7 L), or with good magmatic zoning and corroded rims (Figure 7 M). Eight single zircon or small groups of grains (maximum 3) were analyzed

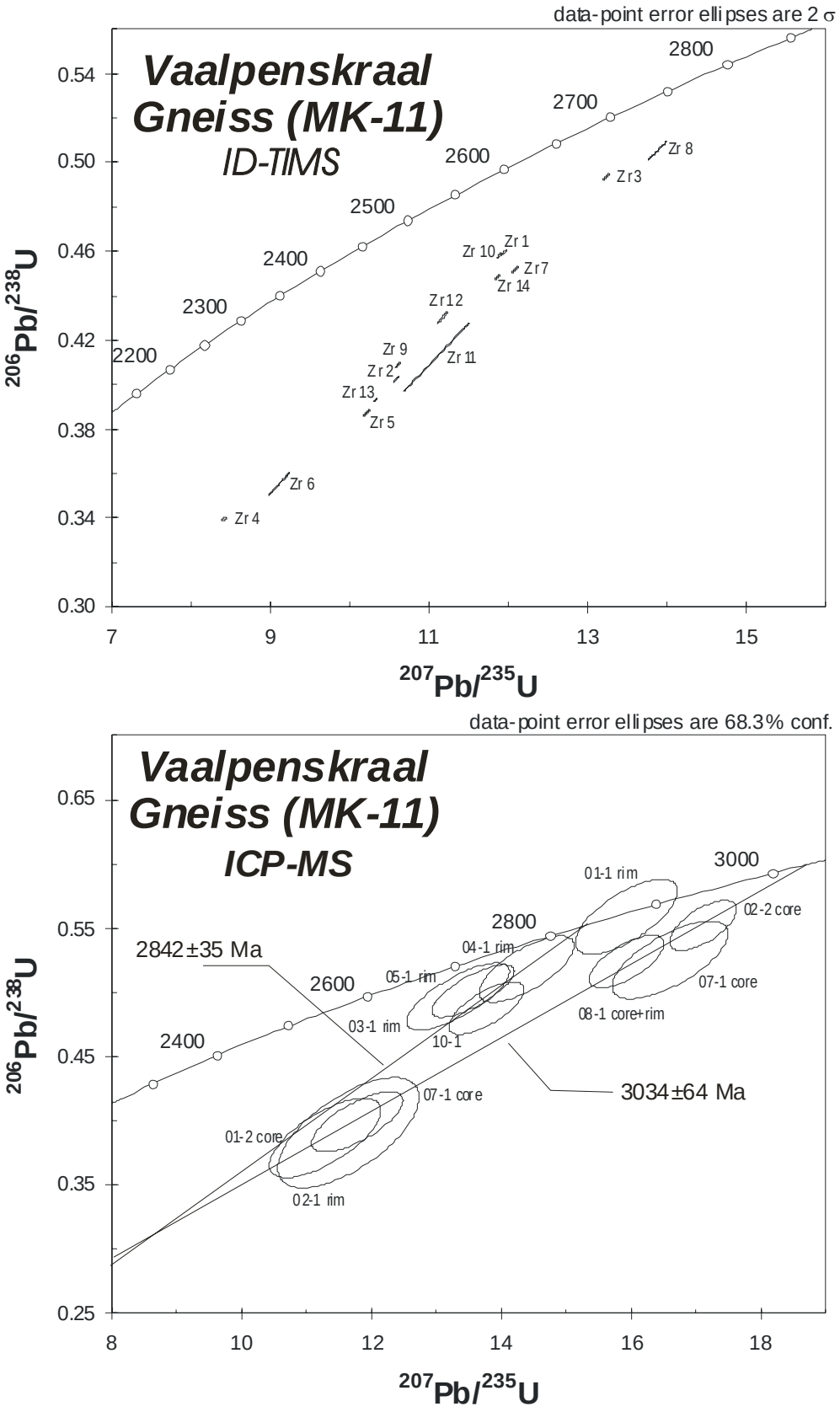

Figure 9. *ID-TIMS and ICP-MS concordia diagrams for Vaalpenskraal-type trondhjemitic gneiss sample MK11.*

(Table 2). Plotted in a concordia diagram (Figure 12, inset) they are discordant to very discordant. The 5 most concordant data define an upper intercept age of 2796.8 ± 2.4 Ma (MSWD=1.7) with a lower intercept at 770 ± 14 Ma (Figure 12). This age of 2800 Ma is regarded as the age of emplacement of this granodiorite.

DISCUSSION

The geochronological study supports the field, petrological and geochemical findings described earlier and provides confirmation of three main periods of magmatic activity within the Makoppa Dome. The oldest rocks recognized so far, the Vaalpenskaal-type trondhjemite gneisses (samples MK10 and MK11), yielded ages identical within error at 3011 +30/-29 Ma and 3034 ± 64 Ma respectively. The Makoppa-type granodiorites/adamellites (sample MK5) was dated at 2886.4 +3/-2.3 Ma while the Rietkuil-type granodiorites (samples MK2 and MK3) gave ages at 2801 ± 24 Ma and 2796.8 ± 2.4 Ma respectively.

With the exception of sample MK5, all the zircons extracted from these samples are characterized by the presence of younger rims/overgrowths. Zircon rims from the trondhjemitic gneisses MK10 and MK11 define ages at 2629 ± 130 Ma and 2842 ± 35 Ma respectively. Unfortunately, the rims on the zircons from the other samples were too small to be dated with the laser beam. It appears therefore that the gneisses (samples MK10 and MK11) were thermally affected either by the emplacement of the Makoppa-type granodiorites/adamellites or the Rietkuil-type granodiorites.

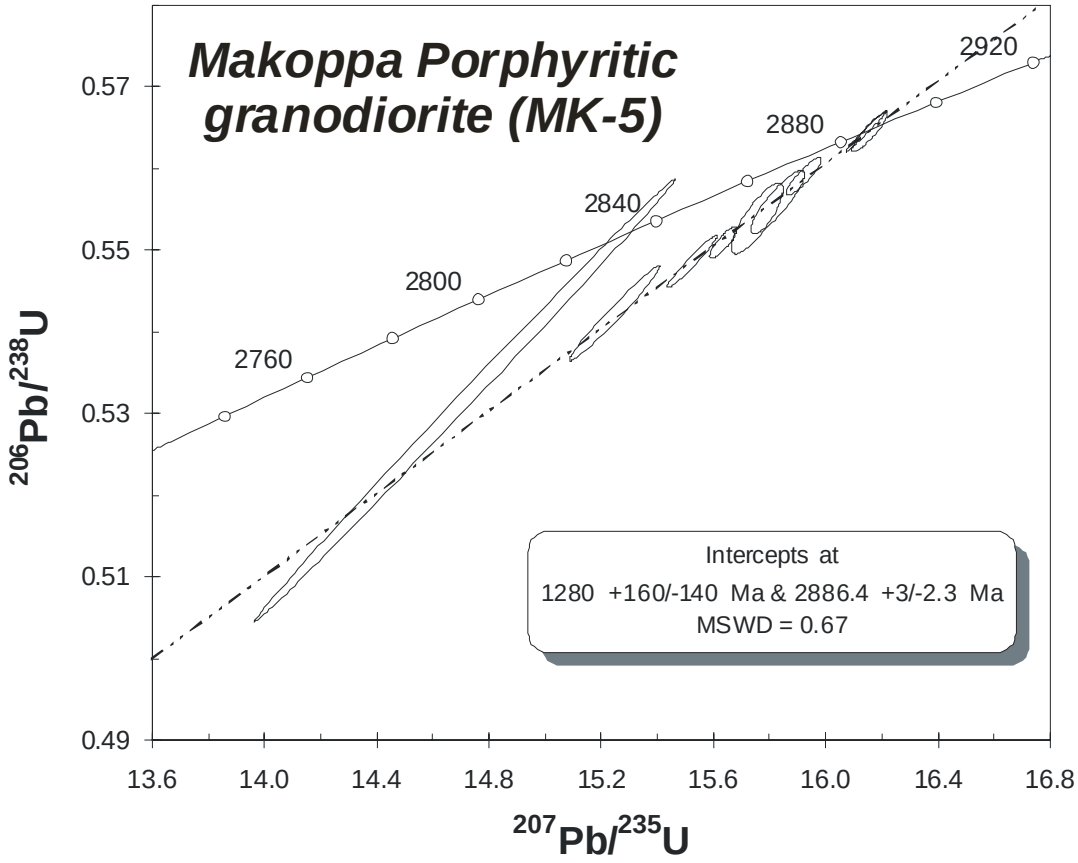

Figure 10. *Concordia diagram for Makoppa-type granodiorite/adamellite sample MK5.*

Another noteworthy feature is that none of the lower intercept ages calculated for the younger samples (MK5: 1280 ± 160 Ma; MK2: 785 ± 60 Ma and MK3: 770 ± 14 Ma) are zero. This is even more remarkable in the case of sample MK2 where LAM-ICP-MS analyses (Figure 11B) plot all the way down the discordia to the point where some zircons are almost concordant at around 800 Ma. Although these dates might not be interpreted as real age(s), their interpretation could be tentatively linked to the presence of the *c.* 1200 Ma Pilanesberg dyke system intruded into the Makoppa Dome.

As discussed in the introduction to this paper the Makoppa granitoid suite has many similarities with Archaean granitoids elsewhere on the Kaapvaal Craton. The mode of occurrence, petrology and geochemical characteristics of the granitoids are remarkably similar in the four domains on the craton defined by Poujol *et al.* (2003) and only their relative ages serve to distinguish them. The geochronological findings clearly indicate that the craton evolved from east to west, with the oldest granitoid suite (*c.* 3600-3200 Ma) being found in the Barberton-Swaziland area, followed westwards by old granite basement in the central Kaapvaal Craton (Johannesburg-Vredefort Domes - *c.* 3340-3000 Ma). Still younger granitoids were produced around the northern, northwestern and western rims of the craton in what has been described as a crescent-shaped juvenile magmatic arc, which initiated approximately 3100-3000 Ma ago (Poujol *et al.,* 2003). On the western and northwestern side of the Kaapvaal Craton these events are manifest in the Kraaipan-Amalia granitoid suite described and dated by Anhaeusser and Walraven (1999) and Poujol *et al*. (2002), and by the findings in the Makoppa Dome region reported in this study. Comparisons of the ages emanating from these two regions are sufficiently coincidental as to confirm their co-genetic evolution in an arc-related setting that existed prior to later continent-arc collision at *c.* 3000-2800 Ma and which produced conditions ideal for the development of foreland basins (such as the Witwatersrand Basin) to the south and east of the collision zone (Poujol *et al*., 2003).

As shown above the Makoppa granitoids show a spread of ages from *c.* 3011 to 2797 Ma. The oldest, the Vaalpenskraal-type, approximates the *c*. 3008 Ma age of the trondhjemitic gneisses in the Amalia area (Poujol *et al*., 2002). The Makoppa-type potassic granitoids dated at *c.* 2886 Ma fall within the range of the *c.* 2915-2879 Ma granodiorites and adamellites found in the central and northern parts of the Kraaipan terrane, and the Rietkuil-type granodiorites dated at *c.* 2797 Ma equate closely with the *c*. 2791 Ma Mosita adamellites, located in the northern Kraaipan terrane (Poujol *et al*., 2002).

The *c*. 2797-2791 Ma ages of the Rietkuil and Mosita granitic rocks also approximate the age of 2785±2 Ma reported by Moore *et al*. (1993) for the Gaborone Granite Suite and Kanye Formation found in Botswana and adjacent areas of northwestern South Africa, again suggesting a possible genetic link (Poujol *et al*., 2002). The distribution of the igneous and volcanic components associated with the Gaborone-Kanye igneous terrane have come under scrutiny in recent years following the availability of Pb-Pb single zircon and precise U-Pb zircon age dating. The Gaborone-Kanye complex is now regarded as having formed during a single magmatic event in the late Archaean evolution of the Kaapvaal Craton (Sibiya, 1988; Grobler and Walraven, 1993; Moore *et al*., 1993; Grobler, 1996).

The basalt, felsic porphyry and lithic tuff succession southeast of Derdepoort, as well as that rimming the Makoppa Dome west of Thabazimbi, has in the past been correlated with the Ventersdorp Supergroup (Jansen *et al*., 1974; Tyler, 1979a). However, the felsic volcanics

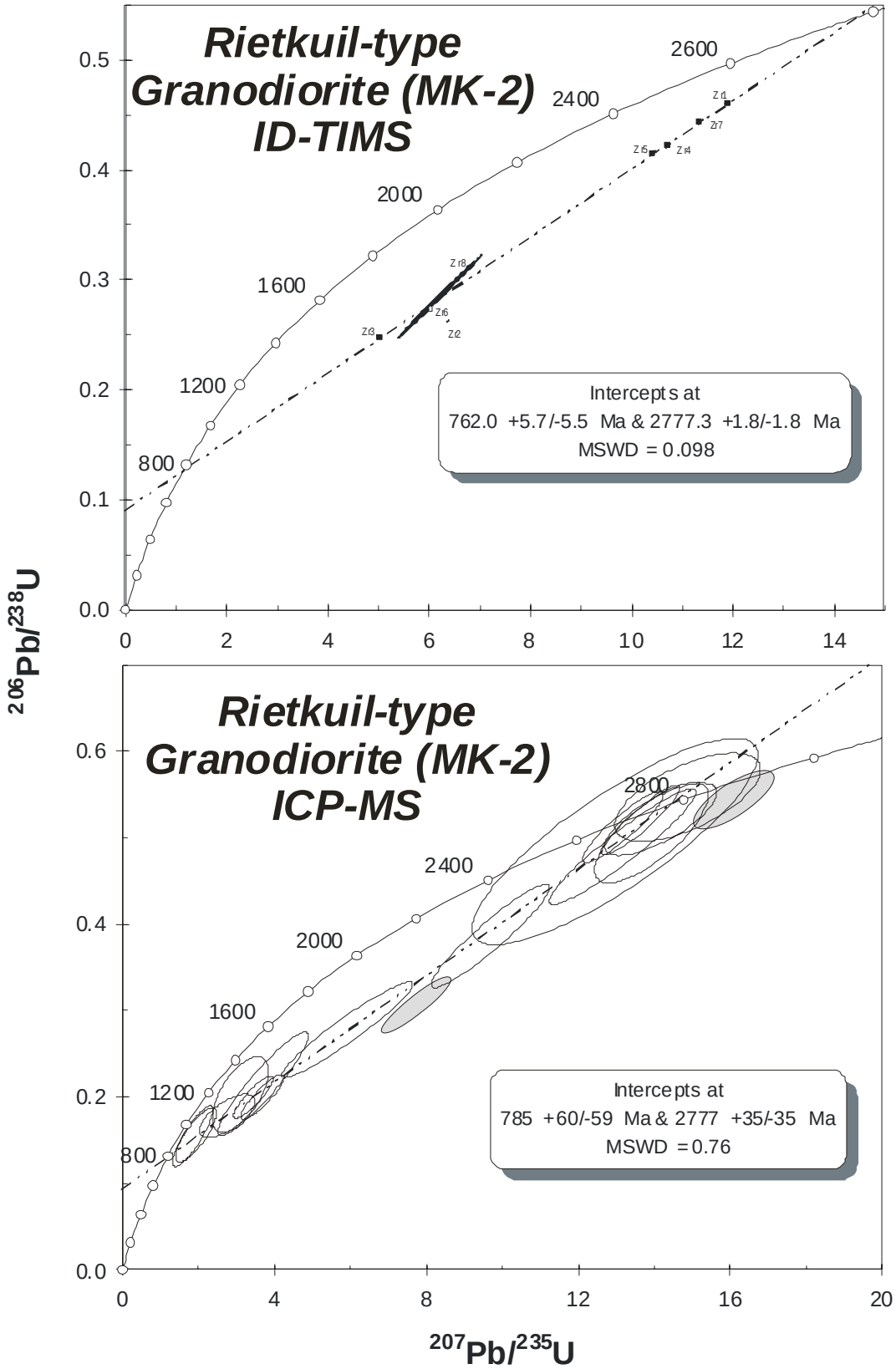

Figure 11. *ID-TIMS and ICP-MS concordia diagrams for Rietkuil-type granodiorite sample MK2.*

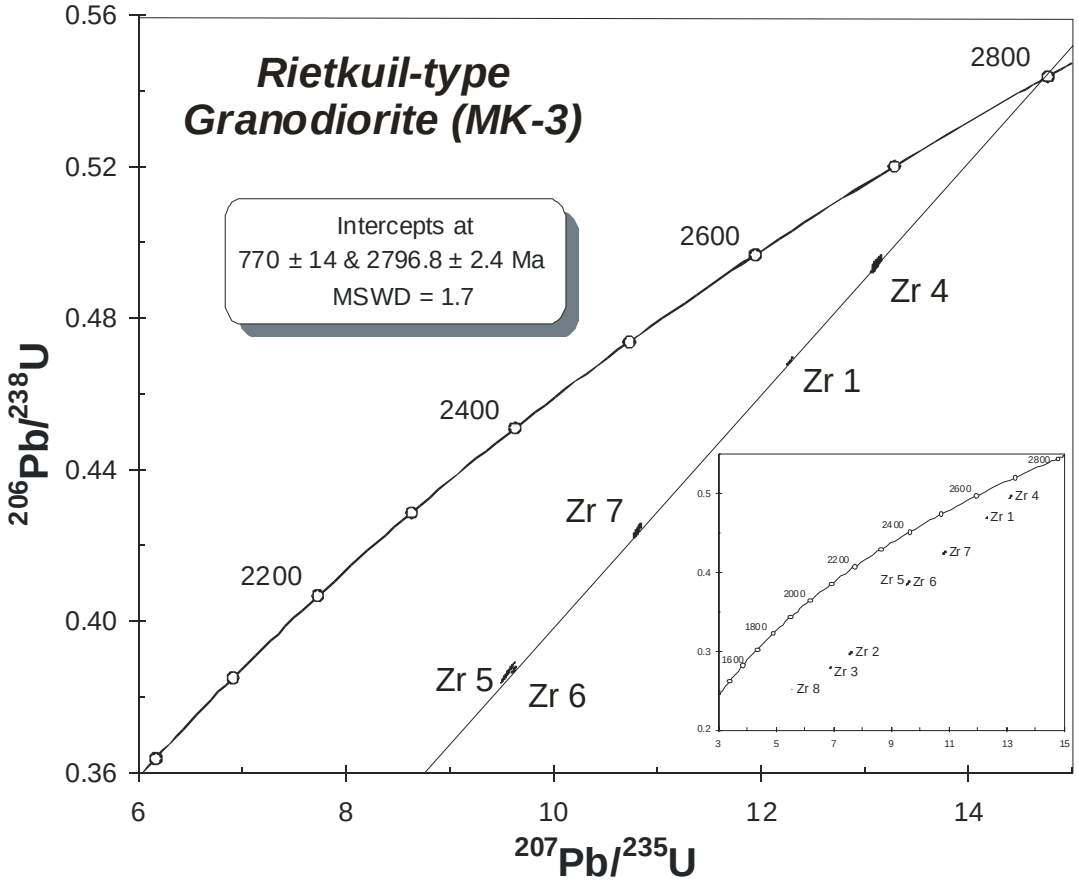

Figure 12. *Concordia diagram for Rietkuil-type granodiorite sample MK3.*

have yielded a concordant SHRIMP U-Pb zircon age of 2781±5 Ma and an age of 2782±5 Ma has been deduced for the eruption of the underlying basalts (Wingate, 1998). These findings render unlikely the correlation of these rocks with the *c.* 2714 Ma Ventersdorp Supergroup age reported by Armstrong *et al*. (1991). The extension of the Gaborone-Kanye complex east of the Botswana border therefore seems a real possibility and provides support for the views that the Kanye volcanic group, in particular, most likely constitutes the proto-basinal (pre-rift) phase of the Ventersdorp Supergroup (Tyler, 1979b; Walraven *et al*., 1994; Grobler, 1996; Wingate, 1998). The distribution of the plutonic phases might equally be more extensive than previously believed with the *c*. 2797 Ma Rietkuil granodiorites possibly being in contention as an early or precursor phase of the *c*. 2785 Ma Gaborone Complex.

The age dating currently available in the northwest Limpopo Province places some constraints on the timing of the development of the Makoppa terrane as a prominent domical feature. An upper limit for the doming must relate to the age of the Waterberg Group, which is regarded by Cheney *et al*. (1990) as having been deposited between 1800-1700 Ma and which appears little affected, structurally, by the doming event in the immediate vicinity of the Makoppa Dome. In the south the Kanye/Ventersdorp/Transvaal successions are all tilted away from the dome, uplift in the north possibly having commenced in post-Rietkuil times (*c.* 2800 Ma). Regionally, however, the main deformation or domical uplift post-dates Transvaal Supergroup sedimentation (*c.* 2642-2224 Ma - Walraven *et al*., 1990; Walraven and Martini, 1995) as well as the adjacent Rustenberg Layered Suite of the Bushveld Complex dated at *c*. 2060 Ma

(Walraven *et al*., 1990). Thus, the main doming of the Makoppa region, as seen today, probably occurred between about 2060 and 1700 Ma and may, in part, be an epeirogenic response to the loading of the crust by the Bushveld Complex.

CONCLUSIONS

Field relationships, as well as petrological, geochemical and geochronological data, have led to the recognition of three geologically distinct granitoid varieties on the Archaean Makoppa Dome of northwest Limpopo Province. Poor exposure, however, makes it impossible to delineate the various granite types on any map of the dome. The earliest variety consists of foliated, Na-rich, trondhjemitic gneisses (Vaalpenskraal-type) that yielded ages ranging between 3034 - 3011 Ma. The trondhjemitic gneisses have been intruded by non-foliated, K-enriched, adamellites and granodiorites (Makoppa-type) that have been dated at *c.* 2886 Ma. These rocks, which are relatively coarse-grained and red in colour in the Makoppa area, occur as grey to white dykes and sheets elsewhere on the dome causing localized potassic metasomatism of the earlier gneisses as well as thermal reheating responsible for the development of zircon overgrowth rims and new zircon grains.

The final phase of granitic magmatism manifest in the region led to the emplacement of homogeneous, grey granodiorites (Rietkuil-type) at *c.* 2801-2797 Ma. This event is closely related time-wise to the emplacement of the Mosita granodiorite in the Kraaipan terrane south of the Botswana border, and both are, in turn, possible precursor granitoids to the *c.* 2785 Ma Gaborone Granite Complex developed in southeastern Botswana.

The Makoppa granitoids have many features in common with those of the Kraaipan-Amalia terrane on the western edge of the Kaapvaal Craton, including similarities in geochemistry, age and geotectonic setting, and supports the contention, outlined by Poujol *et al*. (2003), that a period of Mesoarchaean magmatism was responsible for the development of a major, crescent-shaped arc that accreted onto the northern and western margins of the evolving Kaapvaal crustal fragment at approximately 3100-3000 Ma. This magmatic arc was subjected to the onset of continent-arc collision approximately 3000-2800 Ma, which resulted in the initiation of orogenic conditions around the craton margins and the emplacement locally of collision-related granitoid plutons and numerous post-tectonic granitoid bodies between 2800 to 2690 Ma. Included within the latter time frame was the formation of a large A-type plutonic-volcanic complex (Gaborone granite suite and Kanye Formation) developed on the thickened crust, which subsequently experienced rift-related volcanism responsible for the *c.* 2714-2709 Ma Ventersdorp Supergroup event.

ACKNOWLEDGEMENTS

The following persons assisted CRA with various aspects in the preparation of this paper for publication. Rob Kiefer, Christiano Lana, Sharon Turner, Di du Toit, Lyn Whitfield, Dalena Blitenthall and Lynnette Greyling. Joe Aphane assisted MP with the separation of zircons for isotopic analysis.

REFERENCES

Anhaeusser, C. R. (1973a). The evolution of the early Precambrian crust of southern Africa. *Philosphical Transactions of the Royal Society of London*, **A273**, 359-388.

Anhaeusser, C. R. (1973b). The geology and geochemistry of the Archaean granites and gneisses of the Johannesburg-Pretoria Dome. *Special Publication of the Geological Society of South Africa*, **3**, 361-385.

Anhaeusser, C.R. (1992). Archaean granite-greenstone relationships on the farm Zandspruit 191-IQ, North Riding area, Johannesburg Dome. *South African Journal of Geology*, **95**, 94-101.

Anhaeusser, C. R. (1999). Archaean crustal evolution of the central Kaapvaal Craton, South Africa: evidence from the Johannesburg Dome. *South African Journal of Geology*, **102** (4), 303-322.

Anhaeusser, C. R. (2002a). Report on a field visit to the Makoppa Dome area, northwest Limpopo Province – 20-21 June, 2002. Rep. (Unpubl.), Marlin Granite (Pty) Ltd, Sandton, 11pp.

Anhaeusser, C. R . (2002b). Archaean granitoid rocks of the Makoppa Dome, Limpopo Province, South Africa: preliminary petrological and geochemical results. *Extended Abstract, 11th Quadrennial IAGOD Symposium and Geocongress 2002, Windhoek, Namibia. CD-ROM Geological Survey of Namibia.*

Anhaeusser, C. R. and Burger, A. J. (1982). An interpretation of U-Pb zircon ages for Archaean tonalitic gneisses from the Johannesburg-Pretoria granite dome. *Transactions of the Geological Society of South Africa*, **85**, 111-116.

Anhaeusser, C. R. and Robb, L. J. (1980). Regional and detailed field and geochemical studies of Archaean trondhjemitic gneisses, migmatites and greenstone xenoliths in the southern part of the Barberton Mountain Land, South Africa. *Precambrian Research*, **11**, (3/4), 373-397.

Anhaeusser, C. R. and Robb, L. J. (1981). Magmatic cycles and the evolution of the Archaean granitic crust in the eastern Transvaal and Swaziland. *Special Publication of the Geological Society of Australia*, **7**, 457-467.

Anhaeusser, C. R. and Robb, L. J. (1983a). Geological and geochemical characteristics of the Heerenveen and Mpuluzi batholiths south of the Barberton greenstone belt and preliminary thoughts on their petrogenesis. *Special Publication of the Geological Society of South Africa*, **3**, 131-151.

Anhaeusser, C. R. and Robb, L. J. (1983b). Chemical analyses of granitoid rocks from the Barberton Mountain Land. *Special Publication of the Geological Society of South Africa*, **9**, 189-219.

Anhaeusser, C. R., Robb, L. J. and Viljoen, M.J. (1981). Provisional geological map of the Barberton greenstone belt and surrounding granitic terrane, eastern Transvaal and Swaziland. *Geological Society of South Africa*, Johannesburg.

Anhaeusser, C. R., Robb, L. J. and Viljoen, M.J. (1983). Notes on the provisional geological map of the Barberton greenstone belt and surrounding granitic terrane, eastern Transvaal and Swaziland (1: 250 000 colour map). *Special Publication of the Geological Society of South Africa*, **9**, 221- 223.

Anhaeusser, C. R. and Walraven, F. (1999). Episodic granitoid emplacement in the western Kaapvaal Craton: evidence from the Arcghaean Kraaipan granite-greenstone terrane, South Africa. *Journal of African Earth Sciences*, **28** (2), 289-309.

Armstrong, R.A., Compston, W., Retief, E.A., Williams, I.S. and Welke, H.J. (1991). Zircon ion microprobe studies bearing on the age and evolution of the Witwatersrand Triad. *Precambrian Research*, **53**, 243-266.

Arth, J. G. (1979). Some trace elements in trondhjemites – their implications to magma genesis and paleotectonic setting. *In*: Barker, F. (Ed.) *Trondhjemites, Dacites, and Related Rocks.* Elsevier, Amsterdam, 123-132.

Barker, F. (1979). Trondhjemite: definition, environment and hypotheses of origin. *In*: Barker, F. (Ed.) *Trondhjemites, Dacites, and Related Rocks.* Elsevier, Amsterdam, 1-12.

Barton, J. M. Jr., Barton, E. S. and Kröner, A. (1999). Age and isotopic evidence for the origin of the Archaean granitoid intrusives of the Johannesburg Dome, South Africa. *Journal of African Earth Sciences*, **28**, 693-702.

Bisschoff, A. A. (2000). The geology of the Vredefort Dome (Explanation of Geological Sheets 2627CA, CB, CC, CD, DA, DC and 2727 AA, AB, BA - 1:50 000 scale). *Council for Geoscience*, Pretoria, 49 pp. and map.

Burger, A.J. and Walraven, F. (1979). Summary of age determinations carried out during the period April 1977to March 1978. *Annals of the Geological Survey of South Africa*, **12**, 209-218.

Brandl, G. and Kröner. A. (1993). Preliminary results of single zircon studies from various Archaean rocks of the northeastern Transvaal. *Extended Abstract, 16th International Colloquium of Africa Geology*, Mbabane, Swaziland, 54-56.

Castle, R.O. and Lindsley, D.H. (1993). An exsolution silica-pump model for the origin of myrmekite. *Contributions to Mineralogy and Petrology*, **115**, 58-65.

Cassidy, K. F., Barley, M. E., Groves, D. I., Perring, C. S. and Hallberg, J. A. (1991). An overview of the nature, distribution and inferred tectonic setting of granitoids in the late-Archaean Norseman-Wiluna Belt. *Precambrian Research*, **51**, 51-83.

Cheney, E.S., Barton, J. M. and Brandl, G. (1990). Extent and age of the Soutpansberg sequences of southern Africa. *South African Journal of Geology*, **93**, 664-675.

Clarke, D.B. (1992). *Granitoid Rocks.* Chapman and Hall, London, 283pp.

Council for Geoscience Geophysics Division (CFG) (1975). Total magnetic field intensity map. 1: 250 000 Regional Aeromagnetic Series 2426 Thabazimbi. *Council for Geoscience, Pretoria.*

De Wit, M.J., Roering, C., Hart, R.J., Armstrong, R.A., De Ronde, C. E. J., Green, R. W. E., Tredoux, M., Peberdy, E. and Hart, R.A. (1992). Formation of an Archaean continent. *Nature*, **357**, 553-562.

Drennan, G.R., Robb, L.J., Meyer, F. M., Armstrong, R.A. and De Bruiyn, H. (1990). The nayture of the Archaean basement in the hinterland of the Witwatersrand Basin:II. A crustal profile west of the Welkom Goldfield and comparisons with the Vredefort crustal profile. *South African Journal of Geology*, **93**, 41-53.

Dubé, B., Dunning, G.R, Lauziere, K. and Roddick, J.C. (1996). New in-sights into the Appalachian orogen from geology and geochronology along the Cape Ray fault zone southwest Newfoundland. *Bulletin of the Geological Society of America*,**108**, 101-116.

Frost, B.R., Barnes, C.G., Collins, W.J., Arculus, R.J., Ellis, D.J. and Frost, C.D. (2001). A geochemical classification for granitic rocks. *Journal of Petrology*, **42**, 2033-2048.

Gericke, B. (2001). *New single zircon U-Pb age constraints on the Kraaipan and Amalia granite-greenstone terrane, South Africa: implications for the evolution of the western Kaapvaal Craton.* B.Sc. (Hons.) dissertation (unpubl.), Geology Department, University of the Witwatersrand, Johannesburg, 91pp.

Gibson, R. L. and Reimold, W. U. (2001). The Vredefort impact structure, South Africa: the scientific evidence and a two-day excursion guide. *Memoir of the Geological Survey of South Africa*, **92**, 111pp. *(Council for Geoscience, Pretoria).*

Grobler, D.F. (1996). *The geology, geochemistry and geochronology of the Gaborone Granite Suite and Kanye Formation north of Mafikeng, South Africa.* Ph.D thesis (unpubl.), University of the Witwatersrand, Johannesburg, 457 pp.

Grobler, D.F. and Walraven, F. (1993). Geochronology of Gaborone Granite Complex

extensions in the area north of Mafikeng, South Africa. *Chemical Geology*, **105**, 319-337.

Hart R. J., Welke H. J. and Nicolaysen L. O. (1981). Geochronology of the deep profile through the Archaean Basement of Vredefort, with implications for early crustal evolution. *Journal of Geophysical Research*, **86**, 10663-10680.

Henderson, D.R., Long, L.E. and Barton, J.M. (2000). Isotopic ages and chemical and isotopic compositions of the Archaean Turfloop batholith, Pietersburg granite-greenstone terrane, Kaapvaal Craton. South Africa. *South African Journal of Geology*, **103**, 38-46.

Hunter, D. R. (1970). The Ancient Gneiss Complex in Swaziland. *Transactions of the Geological Society of South Africa*, **73**, 107-150.

Hunter, D.R. (1973). The granitic rocks of the Precambrian in Swaziland. *Special Publication of the Geological Society of South Africa*, **3**, 131-147.

Hunter, D.R. (1974). Crustal deveolopment in the Kaapvaal Craton, I. The Archaean. *Precambrian Research*, **1**, 295-326.

Hunter, D.R., Barker, F. and Millard, H.T. (1978). The geochemical nature of the Archean Ancient Gneiss Complex and Granodiorite Suite, Swaziland: a preliminary study. *Precambrian Research*, **7**, 105-127.

Hunter, D.R., Smith, R.G. and Sleigh, D.W.W. (1992). Geochemical studies of Archaean granitoid rocks in the southeastern Kaapvaal Province: implications for crustal development. *Journal of African Earth Science*, **15**, 127-151.

Jansen, H., Schifano, G. and Schutte, I. C. (Compilers) (1974). Geological map with explanatory notes. *1:250 000 Geological Series 2426 Thabazimbi. Geological Survey of South Africa, Pretoria.*

Kamo, S.L. and Davis, D. W. (1994). Reassessment of Archaean crustal development in the Barberton Mountain Land, South Africa, based on U-Pb dating. *Tectonics*, **13** (1), 167-192.

Kosler, J., Fonneland, H., Sylvester, P., Tubrett, M. and Pedersen, R.B. (2002). U-Pb dating of Detrital zircons for sediments provenance studies – a comparison of laser ablation ICPMS and SIMS techniques. *Chemical Geology*, **182**, 605-618.

Krogh, T.E. (1982). Improved accuracy of U-Pb ages by the creation of more concordant systems using an air abrasion technique. *Geochimica et Cosmochimica Acta*, **46**, 617-649.

Kröner, A., Hegner, E., Wendt, J. I. and Byerly, G.R. (1996). The oldest part of the Barberton granitoid-greenstone terrain, South Africa: evidence for crust formation between 3.5 and 3.7 Ga. *Precambrian Research*, **78**, 105-124.

Kröner, A., Jaeckel, P. and Brandl, G. (2000). Single zircon ages for felsic to intermediate rocks from the Pietersberg and Giyani greenstone belts and bordering granitoid orthogneisses, northern Kaapvaal Craton. *Journal of African Earth Sciences*, **30**, 773-793.

Le Bas, M.J., Le Maitre, R. W. and Woolley, A.R. (1992). The construction of the total alkali-silica chemical classification of volcanic rocks. *Mineral Petrology*, **46**, 1-22.

Lowe, D.R. (1994). Accretionary history of the Archean Barberton greenstone belt (3.55 – 3.22 Ga) southern Africa. *Geology*, **22**, 717-720.

Ludwig, K.R. (1993). A computer program for processing Pb-U-Th isotope data, version 1.24, Denver. United States Geological Survey, Open File Report, **88-542**, 32 pp.

Ludwig, K.R. (2000). Isoplot/Ex: a geochronological toolkit for Microsoft Excel. Berkeley Geochronology Center, Berkeley, California, USA.

Manier, P.D. and Piccoli, P.M. (1989). Tectonic discrimination of granites. *Bulletin of the*

Geological Society of America, **101**, 635-643.
Meyer, F.M., Robb, L.J. Reimold, W.U. and De Bruin, H. (1994). Contrasting low and high Ca granites in the Archaean Barberton Mountain Land, southern Africa. *Lithos*, **32**, 62-76.
Moore, M., Davis, D.W., Robb, L. J., Jackson, M.C. and Grobler, D.F. (1993). Archaean rapakivi granite-anorthosite-rhyolite complex in the Witwatersrand Basin hinterland, southern Africa. *Geology*, **21**, 1031-1034.
Mortimer, C. (1984). Geological map of the Republic of Botswana (1:1 000 000 scale). *Geological Survey of Botswana, Lobatse.*
Moser D. E., Flowers R. M. and Hart R. J. (2001). Birth of the Kaapvaal tectosphere 3.08 billion years ago. *Science*, **291,** 465-468.
Parrish, R.R. (1987). An improved micro-capsule for zircon dissolution in U-Pb geochronology. *Chemical Geology*, **66**, 99-102.
Peacock, M.A. (1931). Classification of igneous rock series. *Journal of Geology*, **39**, 65-67.
Pearce, J.A., Harris, N.B.W. and Tindle, A.G. (1984). Trace element discrimination diagrams for the tectonic interpretation of granitic rocks. *Journal of Petrology*, **25**, 956-983.
Poujol, M. (2001). U-Pb isotopic evidence for episodic granitoid emplacement in the Murchison greenstone belt, South Africa. *Journal of African Earth Sciences*, **33**, 155-163.
Poujol, M. and Anhaeusser, C. R. (2001). The Johannesburg Dome, South Africa: new single zircon U-Pb isotopic evidence for early Archaean development within the central Kaapvaal Craton. *Precambrian Research*, **108**, 139-157.
Poujol, M., Anhaeusser, C. R. and Armstrong, R.A. (2002). Episodic granitoid emplacement in the Archaean Amalia-Kraaipan terrane, South Africa: confirmation from single zircon U-Pb geochronology. *Journal of African Earth Sciences,* **33** (2), 435-449.
Poujol, M. and Robb, L.J. (1999). New U-Pb zircon ages on gneisses and pegmatite from south of the Murchison greenstone belt, South Africa. *South African Journal of Geology*, **102**, 93-97.
Poujol, M., Robb, L.J., Respaut, J.P. and Anhaeusser, C. R. (1996). 3.07-2.97 Ga greenstone belt formation in the northeastern Kaapvaal Craton : implications for the origin of the Witwatersrand Basin. *Economic Geology*, **91**, 1455-1461.
Poujol, M., Robb, L. J., Anhaeusser, C. R. and Gericke, B. (2003). A review of the geochronological constraints on the evolution of the Kaapvaal Craton, South Africa. *Precambrian Research*, **127** (1-3), 181-213.
Robb, L.J. (1983). Geological and chemical characteristics of late granite plutons in the Barberton region and Swaziland with an emphasis on the Dalmein pluton – a review. *Special Publication of the Geological Society of South Africa*, **9**, 153-167.
Robb, L. J. and Anhaeusser, C. R. (1983). Chemical and petrogenetic characteristics of Archaean tonalite-trondhjemite gneiss plutons in the Barberton Mountain Land. *Special Publication of the Geological Society of South Africa*, **9**, 103-116.
Robb, L. J., Anhaeusser, C. R. and Van Nierop, D.A. (1983). The recognition of the Nelspruit batholith north of the Barberton greenstone belt and its significance in terms of Archaean crustal evolution. *Special Publication of the Geological Society of South Africa*, **9**, 117-130.
Robb, L. J., Davis, D. W., Kamo, S.L. and Meyer, F.M. (1992). Ages of altered granites adjoining the Witwatersrand Basin with implications for the origin of gold and uranium. *Nature*, **357**, 677-680
Robb, L.J. and Meyer, F.M. (1987). The nature of the Archaean basement in the hinterland of the Witwatersrand Basin: I. The Rand Anticline between Randfontein and

Rysmierbult. *South African Journal of Geology*, **90** (1), 44-63.
Schmitz, M.D., Bowring, S. A., De Wit, M. J. and Gartz, V. (2003). Subduction and terrane collision stabilize the western Kaapvaal Craton tectosphere 2.9 billion years ago. *Earth and Planetary Science Letters* (in review).
Sibiya, V.B. (1988). *The Gaborone Granite Complex, Botswana, Southern Africa: An Atypical Rapakivi Granite-Massif Anorthosite Association.* Free University Press, Amsterdam, 449 pp.
South African Committee for Stratigraphy (SACS), (1980). Stratigraphy of South Africa. Part 1. (Compiler, L.E. Kent). Lithostratigraphy of the Republic of South Africa, South West Africa/Namibia, and the Republics of Bophuthtswana, Transkei and Venda. *Handbook of the Geological Survey of South Africa*, **8**, 690 pp.
Stacey, J.S. and Kramer, J.D. (1975). Approximation of terrestrial lead isotope evolution by a two stage model. *Earth Planetary Sciences Letters*, **26**, 207-221.
Streckeisen, A. (1976). To each plutonic rock its proper name. *Earth-Science Reviews*, **12**, 1-33.
Tyler, N. (1979a). Stratigraphy, geochemistry and correlation of the Ventersdorp Supergroup in the Derdepoort area, west-central Transvaal. *Transactions of the Geological Society of South Africa*, **82**, 133-147.
Tyler, N. (1979b). Stratigraphy, origin, and correlation of the Kanye Volcanic Group in the west-central Transvaal. *Information Circular, Economic Geology Research Unit, University of the Witwatersrand, Johannesburg*, **130**, 15 pp.
Tyler, N. (1979c). The stratigraphy of the early-Proterozoic Buffalo Springs Group in the Thabazimbi area, west-central Transvaal. *Transactions of the Geological Society of South Africa*, **82**, 215-226.
Van Eeden, O.R., De Wet, N.P. and Strauss, C.A. (1963). The geology of the area around Schweizer-Reneke. An explanation of sheets 2724B (Pudimoe) and 2725A (Schweizer-Reneke). *Geological Survey of South Africa, Pretoria.*
Walraven, F. and Martini, J. (1995). Zircon Pb-evaporation age determinations of the Oaktree Formation, Chuniespoort Group, Transvaal Sequence: implications for Transvaal-Griqualand West basin correlations. *South African Journal of Geology*, **98**, 58-67.
Walraven, F., Armstrong, R.A. and Kruger, F. J. (1990). A chronostratigraphic framework for the north-central Kaapvaal Craton, the Bushveld Complex and Vredefort structure. *Tectonophysics*, **171**, 23-48.
Walraven, F., Retief, E.A. and Moen, H.F.G. (1994). Single-zircon Pb-evaoration evidence for 2.77 Ga magmatism in northwestern Transvaal, Soyuth Africa. *South African Journal of Geology*, **97**, 107-113.
Wingate, M.T.D. (1998). A palaeomagnetic test of the Kaapvaal-Pilbara (Vaalbara) connection at 2.78 Ga. *South African Journal of Geology*, **101**, (4), 257-274.
Witt, W.K. and Davy, R. (1997). Geology and geochemistry of granitoid rocks in the southwest Eastern Goldfields Province. *Western Australia Geological Survey, Report* **49**, 137 pp.
Zimmermann, O. T. (1994). *Aspects of the geology of the Kraaipan Group in the Northern Cape Province and the Republic of Bophuthatswana.* M.Sc thesis (unpubl.), University of the Witwatersrand, Johannesburg, 145 pp.

_____oOo_____